

Leaching of lithium-ion battery materials in sulfate and chloride media for hydrometallurgical recycling

Jere Partinen



Aalto University

Aalto University publication series
Doctoral Theses 28/2025

Leaching of lithium-ion battery materials in sulfate and chloride media for hydrometallurgical recycling

Jere Partinen

A doctoral thesis completed for the degree of Doctor of Science (Technology) to be defended, with the permission of the Aalto University School of Chemical Engineering, at a public examination held at the lecture hall Ke2 of the school on 28 February 2025 at 12 o'clock.

Aalto University
School of Chemical Engineering
Department of Chemical and Metallurgical Engineering

Supervising professor

Associate Professor Mari Lundström, Aalto University, Finland

Thesis advisors

Eng. D. Benjamin P. Wilson, Aalto University, Finland

D.Sc. (Tech) Petteri Halli, Elmery Oy, Finland

Preliminary examiners

Associate Professor Sulalit Bandyopadhyay, NTNU Norwegian University of Science and Technology, Norway

Assistant Professor Shoshan Abrahami, Delft University of Technology, The Netherlands

Opponent

Associate Professor Sulalit Bandyopadhyay, NTNU Norwegian University of Science and Technology, Norway

Aalto University publication series

Doctoral Theses 28/2025

© Jere Partinen

ISBN 978-952-64-2393-7 (soft cover)

ISBN 978-952-64-2394-4 (PDF)

ISSN 1799-4934 (printed)

ISSN 1799-4942 (PDF)

<http://urn.fi/URN:ISBN:978-952-64-2394-4>

Unigrafia Oy

Helsinki 2025

Tekijä Jere Partinen

Väitöskirjan nimi Litiumioniakkumateriaalien liuotus sulfaatti- ja kloridiliuoksissa hydrometallurgisen kierrätyksen osana

Artikkeliväitöskirja

Sivumäärä 60

Avainsanat Litiumioniakkujen kierrätys, Pelkistimet, Sulfaatti–kloridiliuokset, Musta massa

Maailmanlaajuiset pyrkimykset fossiilista polttoaineista puhtaampiin teknologioihin siirtymiseksi ovat kasvattaneet akkujen merkitystä huomattavasti, mikä on arkielämässä näkynyt erityisesti viime vuosina kasvaneena sähköautojen määränä. Sähköautojen litiumioniakut sisältävät suurina pitoisuuksina arvokkaita metalleja, joista monet on määritelty kriittisiksi. Tehokas kierrätys on välttämättömyyden näiden materiaalien saamiseksi takaisin käyttöön niiden elinkaaren lopussa.

Yleisimmin käytetyt akkukierrätysprosessit ovat hydrometallurginen ja pyrohydrometallurginen, joista tämä väitöskirja tutkii hydrometallurgisen prosessin liuotusvaihetta. Liuotuskokeita suoritettiin sulfaatti- ja kloridiliuoksissa käyttäen raaka-aineena niin puhtaita kaupallisia akkukatodikemikaaleja kuin teollisesti prosessoitua akkujätettäkin (musta massa). Nämä raaka-ainevalinnat mahdollistivat sekä puhtaiden katodikemikaalien liuotukseen liittyvien ilmiöiden tutkimisen että muiden akuissa esiintyvien materiaalien liuotusprosessissa aikaansaamien vaikutusten havainnoinnin.

Puhtaiden katodikemikaalien liuotuksessa mangaanin huomattiin saostuvan liuoksesta lämpötiloissa $T \geq 70$ °C ilman lisättyjä pelkistimiä. Vastaavaa saostumista ei havaittu kloridipitoisissa liuoksissa, jotka sen sijaan reagoivat muodostaen kloorikaasua. Lisäksi väitöskirjassa tutkittu liukoisten kuprokloridikompleksien pelkistävää vaikutusta hyödyntävä liuotussysteemi todettiin tehokkaaksi akkukatodimateriaalien liuotuksessa. Systemin avulla saavutettiin yli 90 % Co ja Li saannot suhteellisen miedoissa olosuhteissa (1 M H₂SO₄, 0.2 M NaCl, 30 °C, 2 h). Kokemukset teollisen mustan massan käytöstä raaka-aineena vastaavassa systeemissä herättivät kuitenkin huolta kloridipitoisten liuosten ja mustan massan yhteensopivuudesta reaktioon liittyvän voimakkaan kaasunkehityksen ja vaahdonmuodostuksen vuoksi.

Teollisen mustan massan liuotukseen keskittyvissä tutkimuksissa kuparin pelkistysominaisuuksien havaittiin tehostuvan liuoksen rautapitoisuuden kasvaessa 0.4 g/L Fe asti, kun taas alumiinin pelkistävä vaikutus voimistui ainoastaan lämpötilan noustessa. Lisäksi kuparin havaittiin olevan alumiinia tehokkaampi pelkistin suhteessa näiden metallien luovuttamien elektronien määrään. Kuparin huomattiin myös sementoituvan alumiinikappaleiden pinnalle ja liukenevan uudelleen liuotusprosessin edetessä.

Työssä käytettiin lisäksi Design of Experiments (DoE) -metodologiaa yhdessä regressiomallinnuksen kanssa. Näin saatiin johdettua akkumetallien liuotussaantoja ennustavat yhtälöt perustuen seuraaviin liuotusparametreihin – lämpötila, liuoksen rautapitoisuus sekä kuparin ja vetyperoksidin määrät. Regressioanalyysi osoitti liuoksen rautapitoisuuden ja kuparin määrän olevan katodimateriaalin pelkistymisen kannalta merkittävämpiä tekijöitä kuin usein käytetty H₂O₂, minkä epäiltiin johtuvan useista vetyperoksidiin liittyvistä sivureaktioista.

Aikaisempi akkumateriaalien ja teollisen mustan massan liuotukseen liittyvä kirjallisuus on keskittynyt pitkälti uusien liuotussysteemien kehittämiseen tutkimalla vaihtoehtoisia pelkistimiä vetyperoksidille, mutta teollisen akkujätteen sisältämät metalliset fraktiot ovat tyypillisesti jääneet vähälle huomiolle. Tämä väitöskirja tuottaa uutta tietoa kyseiseltä tieteenalalta tarjoamalla yksityiskohtaisen vertailun sulfaatti- ja kloridiliuoksien liuotustehokkuuksien välillä, esittelemällä uuden kuprokloridikompleksien perustuvan liuotussysteemin ja tutkimalla kuparin ja alumiinin pelkistystehokkuuksia sekä liukoisen raudan roolia elektronien siirrossa näiden metallien ja akkukatodimateriaalien välillä. Tässä väitöskirjassa esitetty tutkimus hyödyttää sekä tulevaa tutkimusta että teollisia akkukierrätystoimijoita tuottamalla lisää tietoa eri liuosten liuotustehokkuudesta sekä akkujätteessä esiintyvien metallisten fraktioiden pelkistystehosta.

Author Jere Partinen

Name of the doctoral thesis Leaching of lithium-ion battery materials in sulfate and chloride media for hydrometallurgical recycling

Article-based thesis

Number of pages 60

Keywords Lithium-ion battery recycling, Reductants, Sulfate–chloride media, Black mass

As a result of the worldwide attempt to phase out fossil fuels and implement cleaner technologies, batteries are becoming increasingly important. One of the most obvious effects of this green transition in everyday life has been the rapid increase in the number of electric vehicles (EVs) over the past few years. Li-ion batteries used in EVs contain high concentrations of valuable materials, many of which are classified as critical. To ensure the circulation of these materials back to reuse after End-of-Life (EoL), efficient recycling is necessary.

The most commonly used battery recycling processes are hydrometallurgical and pyrohydrometallurgical. This thesis studies the leaching step of the hydrometallurgical recycling route. Leaching experiments were performed in sulfate and chloride media, using both pure commercial battery cathode chemicals and industrially processed battery waste – black mass – originating from EoL batteries. This allowed for the investigation of both fundamental phenomena associated with cathode materials leaching as well as holistic process considerations related to the presence of other battery components.

During the leaching of pure cathode chemicals, Mn was observed to precipitate out of sulfate media at temperatures $T \geq 70$ °C in the absence of external reductants. This precipitation was inhibited in chloride-containing lixiviants, where Cl₂ gas was formed instead. Moreover, a system utilizing the reductive properties of soluble cuprous chloride complex species was found to be efficient for battery cathode materials leaching, reaching over 90% Co and Li yields under relatively mild conditions (1 M H₂SO₄, 0.2 M NaCl, 30 °C, 2 h). Nonetheless, observations on the use of real industrial black mass in a similar system raised questions about the compatibility of chloridecontaining lixiviants, as the reactor overflowed due to rapid gas evolution.

In studies involving industrial black mass, the reductive properties of Cu were found to be improved in response to an increased solution iron concentration – up to 0.4 g/L Fe – whereas Al reductive properties were only improved as the temperature was increased. Furthermore, Cu was found to be overall a more efficient reductant in terms of electron efficiency when compared with Al. In the presence of both Cu and Al, copper was also found to temporarily cement on Al particle surfaces and redissolve as leaching progressed.

Furthermore, Design of Experiments (DoE) methodology was used in combination with regression modeling to derive equations that can predict leaching yields based on input parameters – temperature, solution Fe concentration, Cu amount, and H₂O₂ amount. This analysis revealed solution Fe concentration and feed Cu amount as more impactful variables in terms of cathode material reduction when compared with the commonly used hydrogen peroxide. This finding was attributed to the various side-reactions associated with H₂O₂.

Existing literature on LIB cathode material and industrial black mass leaching has largely focused on the development of novel leaching systems by the investigation of alternative reductants to H₂O₂ while often neglecting the role of various metallic components found within industrial black masses. This thesis contributes to the field by providing a detailed comparison of sulfate and chloride media leaching efficiencies, elucidating the capability of soluble cuprous complexes to catalyze the leaching system, and investigating the reductive efficiencies of current collector metals Cu and Al and the role of soluble Fe as an electron transporter between these metals and battery cathode materials. The research presented in this thesis will help future researchers and industrial operators by providing detailed information about the performance of various leaching media and the reductive efficiency of metallic fractions found within industrial black mass.

Acknowledgements

The research in this thesis was conducted at Aalto University, School of Chemical Engineering, Research Group of Hydrometallurgy and Corrosion, Espoo, Finland between 2019 and 2024. The work has been supported by the Finnish Steel and Metal Producers' Fund, Horizon Europe research and innovation programme of the European Union (RESPECT project, grant number 101069865), Business Finland (BATCircle project, grant number 4853/31/2018; BATCircle2.0 project, grant number 44886/31/2020), and ReVolt project (grant number 08_2018_IP167_ReVolt). RawMatTERS Finland Infrastructure (RAMI), funded by the Academy of Finland, is also acknowledged.

I want to thank my supervisor, professor Mari Lundström, for offering me the chance to pursue doctoral studies in her group. I had never seriously thought about becoming a doctoral student before she asked me to consider this opportunity. Taking up the challenge has easily been one of the best decisions of my life, and I have learned and grown so much during these years.

I am grateful to my advisors Dr. Ben Wilson and Dr. Petteri Halli for taking the time and effort to guide me throughout this journey. I have learned so much from them in terms of working in the laboratory and communicating my results in a scientific form. I am also grateful to Docent Jari Aromaa and Prof. Emeritus Olof Forsén for sharing their knowledge about both scientific and other topics at our common coffee breaks. I owe special thanks to Alexander Chernyaev for guiding me during my early steps in the wonderful world of hydrometallurgy, batteries, and laboratory experiments.

I also want to thank my other colleagues from over the years: Sipi Seisko, Antti Porvali, Arman Dastpak, Mika Sahlman, Marja Rinne, Riina Aromaa-Stubb, Anssi Karppinen, Henri Palomäki, Kerli Liivand, Heikki Lappalainen, Diana Arellano, Sonja Nurmi, Sugam Shukla, Zulin Wang, Yuanmin Zou, Reima Herrala, Saeed Rahimpour, Jere Vänskä, Julia Alajoki, and everybody else who has brought joy to the days I have spent in the group.

In addition to my colleagues, I want to thank my father Jarkko and sister Jenni for the continuous love and support at all stages of my life. I could not have wished for a better family. I also want to extend my thanks to my long-standing friend Joonas Tammela for the friendship and countless inside jokes over the years, and for keeping me up to date with pyrometallurgy-related topics.

Espoo, October 30th, 2024
Jere Samuli Partinen

Contents

Acknowledgements	I
List of Publications.....	IV
Author's Contribution	V
1. Introduction	1
1.1 Background	1
1.2 Objectives and scope	3
1.3 New scientific contribution.....	4
1.4 Thesis Structure	6
2. Theoretical Background.....	7
2.1 The lithium-ion battery and its components	7
2.2 Lithium-ion battery recycling methods.....	9
2.2.1 Pre-treatment	10
2.2.2 Pyrometallurgical processing.....	11
2.2.3 Hydrometallurgical processing.....	11
2.2.4 Direct recycling methods	12
2.3 Li-ion battery leaching	13
2.3.1 Sulfuric acid media.....	14
2.3.2 Metallic reductants.....	17
2.3.3 Chloride media	17
2.3.4 Considerations for solution purification	18
2.3.5 Implications of previous literature for the current work	19
3. Experimental.....	21
3.1 Materials and Equipment	21
3.2 Raw material characterization.....	24
3.3 Leaching experiments	25
3.4 Kinetic studies and regression analysis.....	26
4. Results and discussion.....	28
4.1 Leaching of pure Li-ion battery cathode powders	28
4.1.1 Leaching in sulfate and chloride solutions.....	29
4.1.2 Cu as a reductant in the presence of chlorides	33

4.2	Leaching of industrially produced black mass.....	35
4.2.1	Leaching experiments	35
4.2.2	Regression modeling.....	40
4.2.3	Environmental considerations	41
4.2.4	Black mass leaching in the presence of chlorides	42
5.	Critical outlook and future prospects.....	44
6.	Conclusions	46

List of Publications

This doctoral dissertation consists of a summary and the following publications which are referred to in the text by their Roman numerals.

I. Partinen, Jere; Halli, Petteri; Wilson, Benjamin P.; Lundström, Mari. 2023. The impact of chlorides on NMC leaching in hydrometallurgical battery recycling. Elsevier. Minerals Engineering, volume 202, article number 108244. ISSN: 0892-6875. DOI: 10.1016/j.mineng.2023.108244.

II. Partinen, Jere; Halli, Petteri; Helin, Sampsa; Wilson, Benjamin P.; Lundström, Mari. 2022. Utilizing Cu^+ as catalyst in reductive leaching of lithium-ion battery cathode materials in H_2SO_4 -NaCl solutions. Elsevier. Hydrometallurgy, volume 208, article number 105808. ISSN: 0304-386X. DOI: 10.1016/j.hydromet.2021.105808.

III. Chernyaev, Alexander; Partinen, Jere; Klemettinen, Lassi; Wilson, Benjamin P.; Jokilaakso, Ari; Lundström, Mari. 2021. The efficiency of scrap Cu and Al current collector materials as reductants in LIB waste leaching. Elsevier. Hydrometallurgy, volume 203, article number 105608. ISSN: 0304-386X. DOI: 10.1016/j.hydromet.2021.105608.

IV. Partinen, Jere; Halli, Petteri; Varonen, Anna; Wilson, Benjamin P.; Lundström, Mari. 2024. Investigating battery black mass leaching performance as a function of process parameters by combining leaching experiments and regression modeling. Elsevier. Minerals Engineering, volume 215, article number 108828. ISSN: 0892-6875. DOI: 10.1016/j.mineng.2024.108828.

Author's Contribution

Publication 1: The impact of chlorides on NMC leaching in hydrometallurgical battery recycling.

JP: Conceptualization, Methodology, Validation, Formal analysis, Investigation, Data curation, Writing – Original Draft, Visualization. **PH:** Methodology, Validation, Writing – Review & Editing. **BW:** Project administration, Writing – review & editing. **ML:** Conceptualization, Funding acquisition, Project administration, Supervision, Writing – Review & Editing.

Publication 2: Utilizing Cu⁺ as catalyst in reductive leaching of lithium-ion battery cathode materials in H₂SO₄–NaCl solutions.

JP: Conceptualization, Methodology, Validation, Formal analysis, Investigation, Data curation, Writing – Original Draft, Visualization. **PH:** Methodology, Validation, Formal analysis, Writing – Review & Editing, Visualization. **SH:** Investigation. **BW:** Writing – Review & Editing, Project administration. **ML:** Conceptualization, Writing – Review & Editing, Supervision, Project administration, Funding acquisition.

Publication 3: The efficiency of scrap Cu and Al current collector materials as reductants in LIB waste leaching.

AC: Conceptualization, Data curation, Formal analysis, Investigation, Methodology, Validation, Writing – Original Draft. **JP:** Formal analysis, Methodology, Investigation, Writing – Review and Editing. **LK:** Investigation (SEM-EDS analysis), Writing – Review and Editing. **BW:** Writing – Review & Editing. **AJ:** Project administration, Supervision, Writing – Review & Editing. **ML:** Funding acquisition, Project administration, Supervision, Writing – Review & Editing.

Publication 4: Investigating battery black mass leaching performance as a function of process parameters by combining leaching experiments and regression modeling.

JP: Conceptualization, Data curation, Formal analysis, Investigation, Methodology, Validation, Visualization, Writing – Original Draft. **PH:** Writing – Review & Editing. **AV:** Investigation, Writing – Review & Editing. **BW:** Project administration, Writing – Review & Editing. **ML:** Conceptualization, Funding acquisition, Project administration, Supervision, Writing – Review & Editing.

List of Abbreviations and Symbols

Abbreviations

CCF	Central composite face-centered design
D ₂ EHPA	bis(2-ethylhexyl) hydrogen phosphate
DoE	Design of experiments
EDX	Energy-dispersive X-ray spectroscopy
EoL	End-of-life
EU	European Union
EV	Electric vehicle
LCO	Lithium cobalt oxide
LFP	Lithium iron phosphate
LIB	Lithium-ion battery
LMO	Lithium manganese oxide
LTO	Lithium titanate
Ni–Cd	Nickel-cadmium
NiMH	Nickel-metal hydride
NMC	Lithium nickel manganese cobalt oxide
OFAT	One-factor-at-a-time
PLS	Pregnant leach solution
PTFE	Polytetrafluoroethylene
PVDF	Polyvinylidene fluoride
SEM	Scanning electron microscopy
SHE	Standard hydrogen electrode
S/L	Solid-to-liquid ratio
TM	Transition metals

XRD X-ray diffraction

Symbols

$[Al]$	Added aluminum (g)
$[Cl^-]$	Solution chloride-ion concentration (mol/L)
$[Cu]$	Added copper (g)
$[Fe]$	Solution iron concentration (g/L)
$[H_2SO_4]$	Solution sulfuric acid concentration (mol/L)
$[NaCl]$	Solution NaCl concentration (mol/L)
$[T]$	Leaching temperature ($^{\circ}C$)
$[X/TM]$	Molar amount of reductant X in feed divided by the sum of transition metals (Co, Ni, and Mn) molar amounts in feed (mol/mol)
c	Solution metal concentration at sampling interval x (g/L)
k_c	Reaction Rate constant (min^{-1})
m	Mass (g)
m_i	Initial mass of metal in the feed (g)
m_x	Metal loss upon sampling (g)
M_x	Molar mass of element x (g/mol)
m_{xc}	Cumulative metal losses upon sampling prior to sampling interval x (g)
$n_{e (Al/Cu)}$	Relative difference between molar electron amount donated upon Al and Cu dissolution
t	Time (min)
T	Temperature ($^{\circ}C$)
t_f	Total leaching time (min)
t_x	Time at sampling interval x (min)
V_e	Total volume lost upon evaporation (mL)
V_f	Final solution volume after experiment (mL)
V_i	Initial volume (mL)
V_s	Sample volume (mL)
V_{sc}	Cumulative sample volume prior to sampling interval x (mL)
$V_{s tot}$	Total volume of samples during experiment (mL)
x	Dissolved fraction of studied element

Y	Leaching yield
Z_x	Number of electrons donated upon dissolution of one atom of element x
τ	Time required for complete conversion (min)

1. Introduction

1.1 Background

The first modern battery was introduced in 1800 by the Italian physician Alessandro Volta when he reported his findings on his “columnar machine” (Volta, 1800), now known as the voltaic pile. This innovation started the history of contemporary batteries and their development, leading to the discovery of more advanced energy storage systems such as the lead–acid battery (1859), the nickel–cadmium battery (Ni–Cd, 1899), and the nickel–metal hydride battery (NiMH, 1989).

In 1991, the first lithium-ion batteries (LIBs) were introduced to the market (Matsumoto and Gunji, 2022). LIBs exhibited clear advantages over other portable secondary battery chemistries, as they contained no toxic cadmium and possessed a considerably higher energy density than the previous alternatives (Warner, 2015). LIBs also demonstrated a significantly lower self-discharge rate and did not suffer from the memory effect (Manoharan *et al.*, 2024). The importance of the lithium-ion battery for the modern society was later highlighted by the 2019 Nobel Prize in Chemistry which was awarded to scientists John B. Goodenough, M. Stanley Whittingham, and Akira Yoshino for their innovations toward making this technology possible (Nobel Prize Outreach AB, 2024).

The electrochemical properties of LIBs make them an excellent power source for electric vehicles (EV), as they can provide a long driving range with a single charge/discharge cycle. The demand for EVs has recently seen an unprecedented surge – in only five years, the global number of electric passenger cars has increased 8-fold, from 5 million in 2018 to 40 million in 2023 (IEA, 2024). As EVs start to reach their End-of-Life (EoL) – which has been forecast to bring secondary raw material, *i.e.*, waste batteries to circulation on a large scale starting from the second half of the 2030s (IEA, 2024) – LIB recycling is becoming increasingly critical. Recycling will also have a significant role to provide a sufficient raw material supply to battery manufacturers, as several of the battery materials (Li, Ni, Co, Mn, Cu, natural graphite, and phosphate rock) are currently included in the European Union (EU) List of Critical Raw Materials (European Commission, 2023a). However, from a sustainability perspective, recycling should always be the last resort when considering the circularity of materials and products. For example, the circular economy diagram created by Ellen MacArthur Foundation (Ellen MacArthur Foundation, 2021) shows three circular economy steps before recycling: maintain/prolong, reuse/redistribute, and refurbish/remanufacture. For EV batteries, these principles can be followed by

correct charge/recharge habits, reusing the batteries for stationary energy storage applications, and potentially replacing defective modules/cells for fresh ones within the battery pack.

The earliest commercial LIBs were based on the LiCoO_2 (LCO) cathode material, with LiMn_2O_4 (LMO) becoming available shortly afterward (Ehrlich, 2002). However, the current EV industry is mostly using nickel-based chemistries – such as different compositions of the $\text{LiNi}_x\text{Mn}_y\text{Co}_{1-x-y}\text{O}_2$ (NMC) cathode group – due to their higher energy density (IEA, 2024). More recently, an alternative chemistry free of Ni and Co – LiFePO_4 (LFP) – has also gained traction within the EV battery sector, doubling its global share from 20% in 2020 to 40% in 2023 – primarily due to its popularity in China (IEA, 2024).

Of the current LIBs on the market, the chemistries that contain high concentrations of Co and Ni are the most suitable for recycling from an economic point of view, as their material value is significantly higher when compared with, for example, the recently trending LiFePO_4 . Nevertheless, recycling can be incentivized or enforced by legislation to ensure recycling of also lower-value chemistries. An example of such legislation is the EU principle of Extended Producer Responsibility which mandates companies that bring portable batteries to the market to arrange the collection and recycling of these without additional costs to consumers (European Commission, 2023b). Currently, the LIB components that are recycled in modern processes mainly include the metal contents of the batteries – especially Co, Ni, Cu, Mn, and Li – whereas other fractions like graphite, electrolytes, and plastics are often either burned for energy or discarded as waste without further recovery (Latini *et al.*, 2022; Ji *et al.*, 2023).

Recovery targets for the majority of battery metals have been set by the EU in the current battery regulation – 80% for Li and 95% for Co, Cu, and Ni by the end of 2031 (European Commission, 2023b) – however, such targets for Al and non-metallic components are not included, although the topic has recently received significant attention in the scientific field (Cattaneo *et al.*, 2023; Roy *et al.*, 2024; Staudacher *et al.*, 2024). It has been suggested by batteries Europe roadmap for battery raw materials and recycling (European Commission, 2020) that to improve the battery materials recycling, emphasis should be placed on the collection, logistics, sorting, and dismantling steps of the battery recycling process. Moreover, the roadmap suggests that more work should be done to connect metallurgical recycling processes to primary battery manufacturing plants. Finally, it is suggested that all batteries and their production processes should have their environmental impacts assessed with LCA methodology to allow for clearer sustainability evaluations and thereby ensure minimum environmental impacts.

In addition to economic and regulatory issues, recycling operators must also solve numerous technical challenges to ensure the maximal efficiency of their processes – consequently, a comprehensive knowledge of the associated unit processes is crucial. After collection, batteries must be stabilized by, for example, complete discharge after which they can be dismantled and subjected to suitable pre-treatment steps like crushing and sieving in preparation for subse-

quent recycling processes. Current industrially applied battery recycling methods can generally be classified under the categories of hydrometallurgy or pyro-hydrometallurgy, depending on the approach used to extract and recover the constituent materials. Here, the current thesis investigates the phenomena associated with hydrometallurgical processing, where concentrated battery waste “black mass” is subjected to hydrometallurgical treatment, *i.e.*, leaching followed by solution purification and metals recovery. More specifically, this thesis aims to provide new information on the leaching step – both in terms of fundamentals and broader considerations associated with the treatment of real industrially relevant battery waste fractions (black mass).

1.2 Objectives and scope

The field of battery recycling faces various challenges which necessitate the use of carefully planned experimental setups to solve. For example, a thorough understanding of the issues posed by the complex and heterogeneous nature of industrial battery waste necessitates the investigation of such battery waste as raw material and under industrially relevant conditions. In contrast, fundamental research aimed at identifying individual reactions and other phenomena requires a more simplified and well-defined feed free of impurities. To comprehensively cover the topic involving these two aspects, this thesis investigates both fundamental leaching phenomena associated with pure cathode materials as well as the leaching behavior of industrially processed battery waste.

The main goals of this thesis are as follows:

1. To elucidate the phenomena occurring in sulfate and chloride solutions during LIB cathode material leaching in the absence of external reductants (Publication I).
2. To apply a leaching system that utilizes Cu^+ chloride complex species in a novel way to enable efficient electron transfer between metallic copper and battery cathode material, using NaCl as the chloride-ion source (Publication II, Compendium).
3. To investigate the reductive efficiency of battery current collector metals (Cu and Al) toward black mass with different Cu and Al foil amounts (Publication III) and under different temperatures and solution Fe concentrations (Publication IV).
4. To construct regression models able to predict reductive cathode metal leaching yields under various conditions (Publications III and IV).

The topics and publications of this thesis are shown in Figure 1.

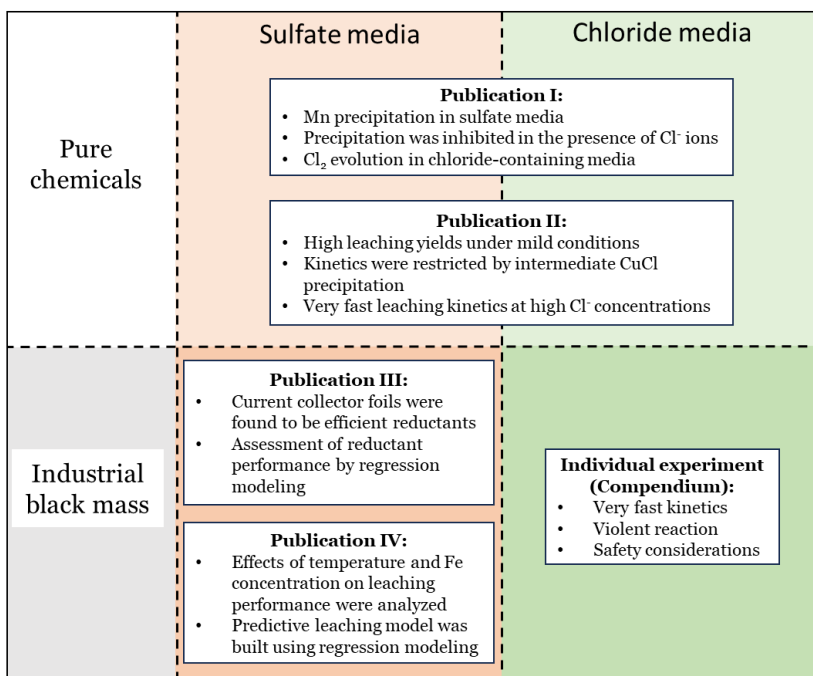


Figure 1. Schematic of the thesis structure with publications, raw materials, and leaching media.

1.3 New scientific contribution

The following findings presented in the publications are proposed as original by the author:

1. A comprehensive comparison between sulfate, chloride, and mixed sulfate–chloride lixivants at different temperatures in the context of pure NMC111-type cathode material leaching was performed. Pure cathode material was used to study the chemical phenomena to avoid any unwanted interference caused by impurities.
 - i. The cathode material delithiation degree was observed to increase as a response to higher leaching temperatures – phases detected within the leach residue included $\text{Li}_{0.4}\text{Ni}_{1/3}\text{Mn}_{1/3}\text{Co}_{1/3}\text{O}_2$ at $T = 30$ °C and a completely delithiated phase, $\text{Mn}_{0.33}\text{Co}_{0.33}\text{Ni}_{0.33}\text{O}(\text{OH})$, at $T \geq 70$ °C.
 - ii. Mn was found to precipitate out of sulfate-based lixivants as a birnessite-type compound – $\text{Li}_4\text{Mn}_{14}\text{O}_{27} \cdot x\text{H}_2\text{O}$ – at 30 °C and MnO_2 at temperatures $T \geq 50$ °C due to the high oxidative power of the investigated battery cathode material.
 - iii. In the presence of Cl⁻ ions, manganese compound precipitation was inhibited, and the anodic reaction of Cl₂ gas evolution dominated instead at temperatures $T \geq 70$ °C.

- iv. Cl_2 gas evolution and the associated cathode material dissolution reaction was more pronounced in H_2SO_4 -NaCl lixivants when compared with HCl.
 2. The leaching system based on cuprous chloride complex species was found to efficiently utilize the reductive properties of metallic Cu toward pure LCO-type cathode material.
 - i. High leaching rates (reaction rate constant $k = 4.6 \cdot 10^{-3} \text{ min}^{-1}$) were obtained with pure cathode material and Cu powder under relatively mild conditions ($T = 30 \text{ }^\circ\text{C}$, $[\text{H}_2\text{SO}_4] = 1 \text{ M}$, $[\text{NaCl}] = 0.2 \text{ M}$) in the presence of 1/1 mol ratio of Cu/LCO.
 - ii. Reaction rates were found to stagnate between 0.2–0.8 M NaCl concentrations due to intermediate CuCl precipitation.
 - iii. CuCl precipitation and the resulting reaction rate stagnation were overcome under chloride concentrations of $[\text{Cl}^-] \geq 1.6 \text{ M}$, resulting in very fast kinetics (reaction rate constant $k \sim 20 \cdot 10^{-3} \text{ min}^{-1}$).
 - iv. To demonstrate this leaching system with industrial NMC111-type black mass representative of typical EV battery waste (Publication IV black mass in Table 3, Section 3), fast kinetics were initially observed (leaching yields of ~60% for Co, Ni, and Mn within 5 min) and rapid gas generation caused the reactor to overflow. However, no significant leaching yield increases were observed upon prolonged leaching.
 3. The individual and combined reductive efficiencies of Cu and Al current collector materials in the leaching of a sieved fraction ($< 500 \text{ }\mu\text{m}$) of an LCO-based black mass (Publication III black mass in Table 3, Section 3) were determined under different temperatures and solution iron concentrations. The black mass fraction in this study was chosen due to its low content in the studied reductant metals Cu and Al, allowing for a more precise investigation of the effects of Cu and Al additions on the system.
 - i. Cu was found to have a higher reductive efficiency (66%) when compared with Al (47%), as a larger share of electrons donated by Cu was utilized in cathode material reduction and dissolution.
 - ii. Al additions to the system resulted in Cu cementation despite the presence of a strong oxidant – *i.e.*, black mass.
 - iii. Al dissolution rate was found to accelerate in response to increased temperatures (40% Al dissolved after 120 min leaching at $T = 30 \text{ }^\circ\text{C}$; 85% Al dissolved at $T = 70 \text{ }^\circ\text{C}$), whereas Cu was not significantly affected by temperature.
 - iv. Cu dissolution rate was observed to increase as the solution iron concentration was increased – up to 400 mg/L Fe – whereas Al was unaffected by Fe concentration.
 4. Design of experiments (DoE) methodology and regression modeling were used to construct models able to predict Co leaching yields from an NMC111-based industrial black mass (Publication IV black mass in Table 3, Section 3) based on temperature, Fe concentration, and additions of Cu, Al, and H_2O_2 . The black mass in this study was chosen due to its lower Fe

content when compared with other black mass types available, which allowed for the systematic study of different soluble Fe concentrations.

- i. The models indicated Cu and Fe additions to be a markedly more efficient method to improve black mass leaching yields when compared to the commonly used H_2O_2 . Increasing the temperature was also found to be an efficient way to improve leaching yields.
- ii. Large differences between the models created in Publications III and IV illustrate the limitations of modeling in leaching processes – models are only valid within the boundaries of investigated parameter values.

1.4 Thesis Structure

This thesis comprises a compendium section as well as four scientific publications (denoted as I, II, III, and IV in the text) appended to the end of the thesis. The compendium part is structured as follows: Chapter 2 reviews the literature related to the scope of the thesis, introducing the parts of a lithium-ion battery along with their functions, current recycling methods for LIBs, and especially the theoretical background related to the leaching step of hydrometallurgical recycling. Chapter 3 lists the chemicals, equipment, and methodology used in the research included in this thesis. Chapter 4 highlights the main results from the publications for discussion, and a critical outlook and future prospects related to the work are outlined in Chapter 5. Lastly, conclusions drawn from the work are presented in Chapter 6.

2. Theoretical Background

This section presents the background of lithium-ion batteries and their components (Section 2.1), along with the most widely used and researched recycling methods and industrial recycling processes (Section 2.2). These subchapters are followed by a comprehensive look at the theory behind leaching of battery cathode materials and industrial black mass (Section 2.3) under the conditions studied in this thesis.

2.1 The lithium-ion battery and its components

Lithium-ion batteries contain various components, each made of different chemical compounds – including organic and inorganic chemicals – tailored to optimize their performance. In order to understand the significance of these materials in the context of a recycling process, it is important to consider the key components contained within batteries and battery packs.

Chemical energy storage within the lithium-ion battery is based on lithium-ion accumulation and transport between the anode and cathode which are separated by a separator – often comprised of polypropylene – to prevent short-circuiting (Figure 2; Or *et al.*, 2020). Both electrodes are composed of substances that can accommodate lithium within their structure. On the cathodic side, lithium-ion storage can be accomplished by a variety of compounds. Layered oxide-type cathode materials – such as LiCoO_2 (LCO) and $\text{LiNi}_x\text{Mn}_y\text{Co}_z\text{O}_2$ (NMC) – store Li ions in between transition metal oxide layers, whereas olivine (LFP) and spinel (LMO) cathode-types store Li ions inside pores within the cathode crystal structure (Harper *et al.*, 2019; Lu *et al.*, 2019). The anode, on the other hand, is typically composed of layered graphite (Castro *et al.*, 2022) which stores Li ions by intercalation between the graphene layers, forming LiC_6 as an intercalation compound (Drüe *et al.*, 2013). In addition to the extensively used graphite, other anode materials have also received a lot of attention in recent research (Hossain *et al.*, 2023). For example, anode doping with Si has been suggested to improve the electrochemical performance of the battery (Bishoyi and Behera, 2024), whereas $\text{Li}_4\text{Ti}_5\text{O}_{12}$ (LTO) has found a lot of interest due to its superior performance regarding safety and fast-charging characteristics when compared with graphite-based anodes (Gopalakrishnan *et al.*, 2016).

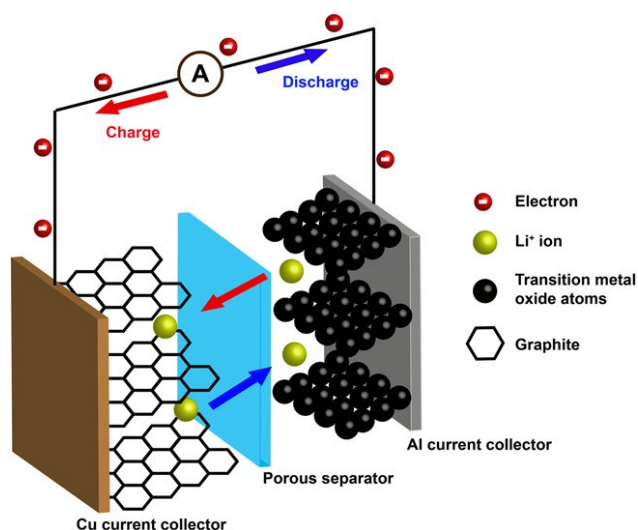


Figure 2. Main components of the lithium-ion battery and illustration of the charge–discharge cycle. Adopted from Or *et al.*, 2020. Reproduced from Wiley under CC BY 4.0.

In a fully charged state, all the lithium is stored at the anode, and upon discharge, lithium ions migrate to the cathodic side of the battery, resulting in electron transfer – *i.e.*, electric current – through an external circuit (Warner, 2015). Li-ion transfer between the anode and cathode is enabled by the electrolyte, which is typically an organic solvent like ethylene carbonate or dimethyl carbonate, with a lithium-containing salt – often LiPF_6 – dissolved within (Liu *et al.*, 2023). To allow for electric current passage through an external circuit, electrode active materials are attached to metallic current collectors – Cu for the anode, Al for the cathode – which collect the electric charge released upon Li-ion transfer and conduct it to power a desired application (Zhu *et al.*, 2021). Electrode material adhesion on current collector surfaces is achieved with a binder – often polyvinylidene fluoride (PVDF) – the choice of which may also affect the solid–electrolyte interphase formation and electrode charge transfer capabilities (Trivedi *et al.*, 2024).

In EVs, the materials mentioned above are packed within cells inside a casing typically made of nickel-coated steel (cylindrical cells) or aluminum (pouch and prismatic cells) (Bree *et al.*, 2023). These cells are further packed into modules, which together with the casing material (*e.g.*, steel, aluminum, plastics, fiber glass, or composite materials), battery management system, and electrical connections constitute the battery pack (Figure 3; Warner, 2015).

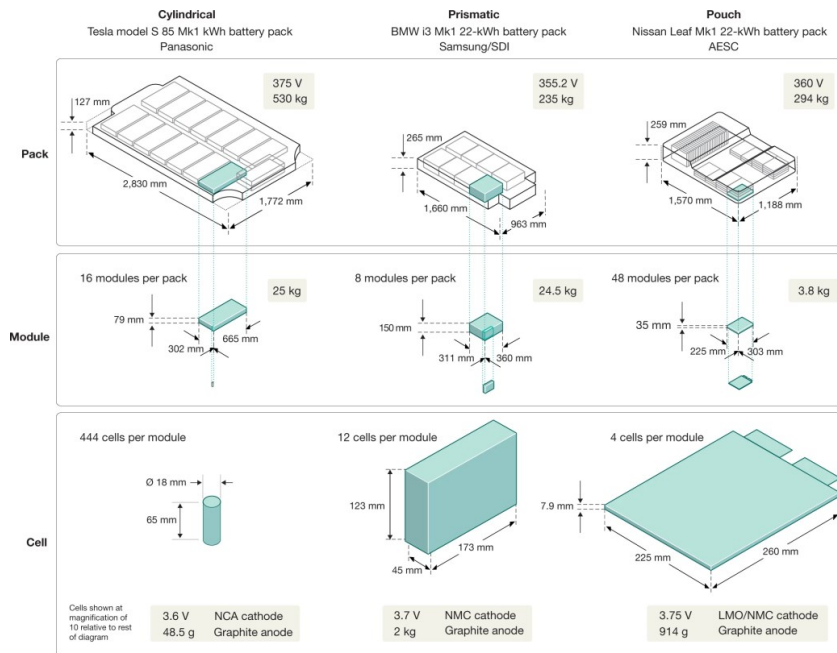


Figure 3. Construction of EV battery packs from cylindrical, prismatic, and pouch cells. Adopted from Harper *et al.*, 2019 with permission. © Springer Nature.

2.2 Lithium-ion battery recycling methods

Despite the importance of recycling as a tool to enable material circulation back to primary production at battery end-of-life (EoL), it is important to consider other alternatives – maintain/prolong, reuse/redistribute, and refurbish/re-manufacture (Ellen MacArthur Foundation, 2021) – for as long as the battery state-of-health allows. Particularly, reuse – as detailed in the European Union Waste Framework Directive (European Commission, 2024) – should be prioritized to ensure a maximal lifetime for the materials and other resources used in the manufacture of the product. EV batteries can often be used in stationary energy storage applications after their capacity is no longer sufficient for use in EVs, that not only results in prolonged battery use, but also potentially reduced environmental impacts over whole battery lifetime (Kang *et al.*, 2025).

After reuse is no longer possible, EoL batteries must be recycled to reclaim their valuable materials and bring them back to circulation. The complex structure of such batteries and the multitude of components contained within necessitate the development of flexible recycling processes able to handle a wide variety of battery designs and chemistries. The main industrially used recycling methods can be divided into pyrometallurgical, hydrometallurgical, and mechanical separation methods. Although these recycling methods are often discussed separately in literature – sometimes even with an inferred intent to show the supremacy of one over the other – none of them is alone able to recycle batteries back into pure substances or battery-grade chemicals to produce new batteries. In fact, these processes are complementary rather than competing, and

are always used in combination in one way or another. Before subjecting EoL battery waste to recycling processes, batteries often must undergo battery pack sorting and disassembly to remove casing materials and expose battery cells for subsequent processing (Velázquez-Martínez *et al.*, 2019). This disassembled material first undergoes pre-treatment and subsequently to metallurgical recycling processes. Alternatively, the battery waste can be subjected directly to a pyrometallurgical process without need for further pre-treatment (Figure 4).

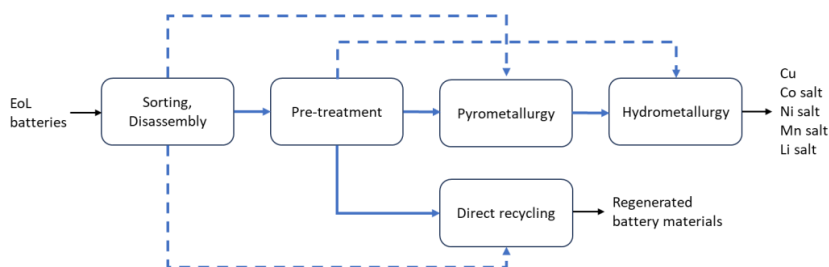


Figure 4. A simplified schematic of different battery recycling process options and products.

2.2.1 Pre-treatment

Commonly, battery cells are stabilized before recycling to avoid explosion risks and fire hazards. A popular stabilization method used in scientific research is complete battery discharge, often achieved by attachment to an external circuit or immersion in a brine solution – *e.g.*, NaCl (Amalia *et al.*, 2023; Shi *et al.*, 2023). In established industrial processes, however, discharge is often circumvented by performing the primary crushing or shredding stage under an inert atmosphere such as carbon dioxide, argon gas, or water spray (Harper *et al.*, 2019). However, such alternative stabilization methods are unable to recover any residual electric energy from EoL batteries – a topic that has previously been highlighted, for example, in the European Commission Batteries Europe Roadmap (European Commission, 2020).

After sorting, disassembly, and stabilization, waste batteries are typically subjected to various mechanical separation methods to separate battery fractions into individual material streams. There are multiple ways to achieve efficient separation, but an example presented by Mossali *et al.* (2020) is briefly discussed here. Typically, the battery cells are first crushed to allow for steel casing removal by magnetic separation. The crushed battery waste then continues to a finer grinding stage to detach electrode powders from current collectors and separate these into different streams by sieving. The overflow – comprising mostly plastics and metallic materials – can then be subjected to eddy current separation and densimetric methods to separate Cu, Al, and plastics and direct them to dedicated recycling processes. The underflow – the fine fraction containing the electrode active materials (*i.e.*, black mass) – can then be subjected to subsequent recycling processes such as hydrometallurgical or pyrometallurgical recycling.

Pre-treatment processes can also include thermal treatments, *e.g.*, electrolyte evaporation and plastics pyrolysis (Makuza *et al.*, 2021). High-temperature treatments can also help in binder removal and purify the raw material for subsequent metallurgical processes. Electrolyte recovery from battery waste has also been investigated – primarily via supercritical CO₂ treatment (Roy *et al.*, 2024).

2.2.2 Pyrometallurgical processing

Pyrometallurgical processes include various methods involving thermal treatment. These processes rely on elevated temperatures to achieve various phase transitions, structural changes, and chemical reactions within the black mass, *e.g.*, cathode material smelting and reduction. Some pyrometallurgical recycling processes – such as the one developed by Umicore – can also treat whole batteries by smelting, with only minimal dismantling requirements (Velázquez-Martínez *et al.*, 2019). Smelting produces two immiscible molten phases – a metallic alloy containing Cu, Co, Ni, and a fraction of Fe, and an oxidic slag phase containing Al, Mn, Li, and the rest of the Fe.

The greatest advantages of pyrometallurgical processes include simplicity, good scalability and high flexibility toward different battery types and chemistries (Liu, C. *et al.*, 2019). The main disadvantages – especially in the case of smelting – have been claimed to be the high energy usage associated with the method and loss of lithium into slag, which may necessitate further slag treatment by, *e.g.*, hydrometallurgical methods (Cornelio *et al.*, 2024). Hence, these treatment methods are typically combined into a pyro-hydrometallurgical recycling process, where smelting is followed by hydrometallurgical metals recovery and refining. Nonetheless, the shortcomings mentioned above may not be common between all pyrometallurgical processes, as *e.g.* Umicore claim their process achieves over 70% Li recovery from the fumes formed during smelting, while additionally producing excess energy by the combustion of the carbon content (Umicore, 2023; Scheunis and Callebaut, 2024). This characteristic, however, underlines another potential drawback of pyrometallurgical processes, as any carbon-containing materials in the feed are burned for energy, resulting in a complete loss of plastic fractions and graphite materials (Latini *et al.*, 2022).

2.2.3 Hydrometallurgical processing

Hydrometallurgical processing can be used to reclaim valuable metals from mechanically pre-treated black mass or metal-containing fractions produced by pyrometallurgical treatment (Yasa *et al.*, 2023). Hydrometallurgical recycling methods use multiple unit processes to transfer metals into soluble form and recover them one by one as high-purity products. The first step of hydrometallurgical processing is leaching, where soluble compounds are transferred into solution form for further purification and recovery, whereas the leach residue – comprising mainly graphite, plastics, and binder materials – is typically burned or landfilled (Liivand *et al.*, 2023). Leaching is most often performed using an

inorganic acid – especially H_2SO_4 – as the lixiviant and hydrogen peroxide as a reductant (Harper *et al.*, 2019). Due to concerns related to chemical and environmental footprints, a plethora of research on alternative acids and reductants has been conducted (Jena *et al.*, 2021; Castro *et al.*, 2022; Li *et al.*, 2024). Leaching will be discussed in more detail in Section 2.3.

After solubilization, the pregnant leaching solution (PLS) undergoes a series of separation and recovery steps for metals reclamation and valorization (He *et al.*, 2024). Co, Ni, and Mn are often separated from PLS by solvent extraction – typically using bis(2-ethylhexyl) hydrogen phosphate (D2EHPA) and Cyanex 272 (Jantunen *et al.*, 2022). After separation, Co, Ni, and Mn can be recovered by *e.g.* precipitation, crystallization, or electrowinning (Larouche *et al.*, 2020). Regarding current collectors and casing metals, copper can be recovered by cementation with iron powder, sulfide precipitation, or hydroxide precipitation (Schlesinger *et al.*, 2022), while iron and aluminum can be removed by solution neutralization, producing $\text{Fe}(\text{OH})_3$ and $\text{Al}(\text{OH})_3$ (Wang and Friedrich, 2015) or phosphate precipitates (Chernyaev *et al.*, 2023; Zou *et al.*, 2024). Lithium is typically the last metal to be recovered from solution, often by precipitation as *e.g.* Li_2CO_3 or LiOH (Zhang *et al.*, 2020). Nonetheless, due to the expected increase in Li demand and potential future supply shortages, solvent extraction of lithium from PLS as the first element or directly after Ni and Co separation has also been studied lately (Zhang *et al.*, 2020; Wesselborg *et al.*, 2021). Early-stage Li recovery is suggested to mitigate Li losses typically associated with solution purification and other metals recovery steps, albeit the competitive extraction mechanism between Li^+ and H^+ ions may potentially pose drawbacks (Wesselborg *et al.*, 2021). In traditional industrial recycling processes, the recovery of Li and Mn has often been overlooked, however, the methods described above are technologically viable and being applied in new industrial processes – as indicated by recent patents related to Li and Mn recovery (Harris and White, 2021; Kivelä *et al.*, 2023).

2.2.4 Direct recycling methods

In addition to the processes described above, direct recycling methods for batteries have also been developed. Direct recycling as a term is not strictly defined but is commonly used to describe battery materials reuse without the involvement of extensive thermal or chemical treatments (Figure 4; Ji *et al.*, 2023). Typically, batteries undergo similar pretreatment steps as with traditional recycling processes. In these processes, Battery components – such as cathode materials or graphite – are then separated and reclaimed for potential reuse. For example, selective flocculation in combination with froth flotation has recently been investigated as a potential separation method (Rinne *et al.*, 2024).

Due to the various structural changes undergone by the cathode and anode materials during their lifetime, the separated battery components typically require an additional regeneration step before they can be used in new battery cells (Xu *et al.*, 2023). Anode materials require different approaches when compared with cathode chemicals, and the optimal regeneration method also varies from

one material to another, necessitating the development of a vast array of regeneration methods (Ji *et al.*, 2023).

The proposed advantages of direct recycling when compared to traditional pyro- and hydrometallurgical processes include preservation of the material structure and morphology, energy efficiency, cost effectiveness, and easy scale-up. Nonetheless, it has been suggested that direct recycling of EoL batteries may not be industrially viable with current technological capabilities, and the method will likely be more suitable for treating production scraps, as such materials have not been packed into complex battery packs or subjected to various aging-related transformations (Hayagan *et al.*, 2024). Notwithstanding, promising results have recently been achieved with respect to graphite recovery from black mass leach residues and its reuse in new battery cells (Chernyaev *et al.*, 2024) and electrocatalysts (Liivand *et al.*, 2023), indicating potential benefits in the application of direct recycling methods in combination with traditional hydrometallurgical processes.

2.3 Li-ion battery leaching

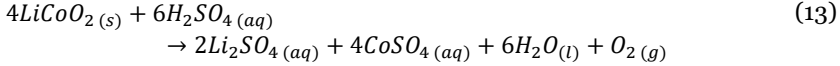
This subsection describes the phenomena that occur during LIB leaching in sulfate and chloride media, as well as the reactions associated with reductants relevant to this thesis. It is important to note that this thesis primarily deals with cathode chemistries that have a layered structure – such as LCO and NMC. Therefore, this subchapter only considers the reactions associated with these specific cathode materials and excludes other materials – like LiFePO₄ – which have different mechanisms associated with their dissolution. A list of half-cell reactions relevant in the context of this thesis is presented in Table 1.

Table 1. Half-cell reactions relevant to the thesis along with their reduction potentials, calculated with HSC 9.4.1 at 30 °C.

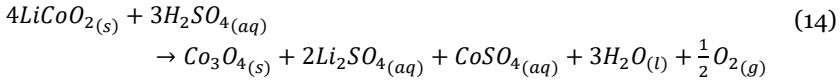
Half-cell reaction	E (V vs. SHE)	Eq. (#)
$\text{LiCoO}_{2(\text{s})} + 4\text{H}^{+}_{(\text{aq})} + \text{e}^{-} \rightarrow \text{Li}^{+}_{(\text{aq})} + \text{Co}^{2+}_{(\text{aq})} + 2\text{H}_2\text{O}_{(\text{l})}$	2.152	1
$\text{O}_{2(\text{g})} + 4\text{H}^{+}_{(\text{aq})} + 4\text{e}^{-} \rightleftharpoons 2\text{H}_2\text{O}_{(\text{l})}$	1.225	2
$2\text{H}^{+}_{(\text{aq})} + \text{O}_{2(\text{g})} + 2\text{e}^{-} \rightleftharpoons \text{H}_2\text{O}_{2(\text{aq})}$	0.690	3
$\text{H}_2\text{O}_{2(\text{aq})} + 2\text{H}^{+}_{(\text{aq})} + 2\text{e}^{-} \rightleftharpoons 2\text{H}_2\text{O}_{(\text{l})}$	1.761	4
$\text{MnO}_{2(\text{s})} + 4\text{H}^{+}_{(\text{aq})} + 2\text{e}^{-} \rightleftharpoons \text{Mn}^{2+}_{(\text{aq})} + 2\text{H}_2\text{O}_{(\text{l})}$	1.227	5
$\text{Cl}_{2(\text{g})} + 2\text{e}^{-} \rightleftharpoons 2\text{Cl}^{-}_{(\text{aq})}$	1.355	6
$\text{Cu}^{2+}_{(\text{aq})} + 2\text{e}^{-} \rightleftharpoons \text{Cu}_{(\text{s})}$	0.337	7
$\text{Cu}^{2+}_{(\text{aq})} + \text{e}^{-} \rightleftharpoons \text{Cu}^{+}_{(\text{aq})}$	0.160	8
$\text{Cu}^{+}_{(\text{aq})} + \text{e}^{-} \rightleftharpoons \text{Cu}_{(\text{s})}$	0.515	9
$[\text{CuCl}_2]^{-} + \text{e}^{-} \rightleftharpoons \text{Cu}_{(\text{s})} + 2\text{Cl}^{-}_{(\text{aq})}$	0.189	10
$\text{Fe}^{3+}_{(\text{aq})} + \text{e}^{-} \rightleftharpoons \text{Fe}^{2+}_{(\text{aq})}$	0.644	11
$\text{Al}^{3+}_{(\text{aq})} + 3\text{e}^{-} \rightleftharpoons \text{Al}_{(\text{s})}$	-1.698	12

2.3.1 Sulfuric acid media

LIB black mass leaching is typically carried out in sulfuric acid (Harper *et al.*, 2019) due to its low price, good availability, and widespread industrial application (Müller, 2000). During the leaching process, hydrogen ions react with LIB cathode metal oxides, solubilizing the cathode metals and producing water and oxygen gas as a result (Equation 13; Nan *et al.*, 2005). This dissolution has been attributed to the ability of cathode metal oxides to oxidize water to O_2 gas and H^+ ions (Equations 1 and 2 in Table 1; Cerrillo-Gonzalez *et al.*, 2020). However, to the knowledge of the author, no experimental verification in favor of this mechanism has been presented in previous literature.

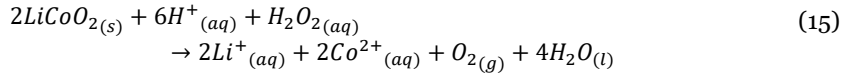


Nevertheless, in the absence of external reductants, the above-mentioned reaction typically does not proceed to completion. Instead, the leaching progress tends to stall after around 40–60% of the cathode transition metals have been leached (Sohn *et al.*, 2006; Takacova *et al.*, 2016; Porvali *et al.*, 2020a). This stagnation has been hypothesized to be caused by structural changes in the cathode material – like formation of Co_3O_4 (Equation 14) in the case of LCO (Ferreira *et al.*, 2009) and other highly oxidized transition metal oxides in the case of NMC (Billy *et al.*, 2018) – as such oxides exhibit semiconductor-like properties (Ma *et al.*, 2019), that hinder electron transfer to the cathode material.



In contrast, Li dissolution is not as strongly controlled by these principles – when compared to transition metals Co, Ni, and Mn – as Li ions can deintercalate from the cathode metal oxide structure without such requirement for electrons, *i.e.*, reductants. This deintercalation subsequently results in the formation of delithiated cathode material compositions such as $Li_{0.62}CoO_2$ and $Li_{0.49}CoO_2$ in the case of LCO (Takacova *et al.*, 2016) and $Li_{0.48}Mn_{0.33}Co_{0.33}Ni_{0.33}O_2$ and $Li_{0.38}Mn_{0.33}Co_{0.33}Ni_{0.33}O_2$ in the case of NMC (Billy *et al.*, 2018). Furthermore, it has been suggested that this deintercalation reaction may release electrons which can further contribute to cathode material reduction and dissolution (Billy *et al.*, 2018) – potentially also facilitating the partial cathode material dissolution mentioned above.

Regardless of the mechanism governing the initial dissolution step, the high transition metal oxidation states in layered oxide-type cathode materials (Co^{3+} , Ni^{2+} , Mn^{4+} ; Shinova *et al.*, 2008) necessitate the presence of a reductant, as higher-valence ions such as Co^{3+} and Mn^{4+} are not stable in aqueous solutions. The most widely used and researched reductant for LIB cathode materials is hydrogen peroxide (Harper *et al.*, 2019; Mao *et al.*, 2022) which dissociates into oxygen gas and water as a result of the reaction with cathode materials (Equation 15).



Although several other processes use H_2O_2 as an oxidant due to its high oxidation potential (Equation 4 in Table 1), the superior oxidative properties of battery cathode materials allow for the use of peroxide as a reductant (Equation 3 in Table 1) in LIB leaching. Nevertheless, hydrogen peroxide production is associated with a high energy consumption and toxic by-products generation (Che *et al.*, 2022), which makes it a suboptimal reductant from an environmental impact perspective. Another drawback associated with H_2O_2 is the presence of metallic components within black masses, as peroxide readily oxidizes Cu, Al, and Fe, diminishing the reductive power of both H_2O_2 and these metals (Chernyaev *et al.*, 2022). Moreover, H_2O_2 decomposition has been reported to be accentuated in the presence of dissolved Fe (Gil-Lozano *et al.*, 2017), and even more so in the presence of both soluble Fe and Cu (Eul *et al.*, 2001). Furthermore, the reduction of H_2O_2 to water via Cu or Al oxidation also increases the acid consumption of the process (Equation 4 in Table 1). To overcome these drawbacks, a plethora of research with the aim to find alternative and novel reductants as a replacement for H_2O_2 has been conducted (Table 2).

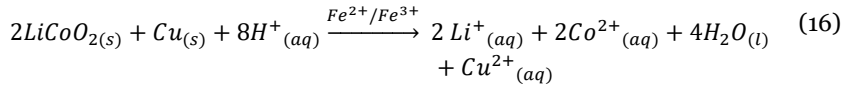
Table 2. An overview of LIB leaching systems studied in literature.

Lixiviant + reductant	Temperature	Leaching yields	Reference
2 M H_2SO_4 , 10 vol-% H_2O_2	75 °C	99% Co	Sohn <i>et al.</i> , 2006
2.5 M H_2SO_4 , 0.8 M NH_4Cl	80 °C	99% Li; 97% Co, Ni, Mn	Lv <i>et al.</i> , 2018
3 M H_2SO_4 , 0.4 g/g glucose/LCO powder	95 °C	96% Li; 98% Co	Chen <i>et al.</i> , 2018
3 M H_2SO_4 , 0.4 g/g sucrose/LCO powder	95 °C	100% Li; 96% Co	Chen <i>et al.</i> , 2018
2 M H_2SO_4 , 0.3 g/g waste tea biomass/LIB cathode powder	90 °C	> 90% Li, Co, Ni, Mn	Chen <i>et al.</i> , 2019
1M H_2SO_4 , 1.2 g/g Cu/NMC powder	30 °C	99% Li, Co, Ni, Mn	Joulié <i>et al.</i> , 2017
2 M H_2SO_4 , 0.11 M ascorbic acid	80 °C	96% Li; 94% Co	Peng <i>et al.</i> , 2018
4 M Formic acid	60 °C	80% Li; 50% Co	Gao <i>et al.</i> , 2017
2 M H_2SO_4 , 15 vol-% H_2O_2	75 °C	100% Li, Co	Shin <i>et al.</i> , 2005

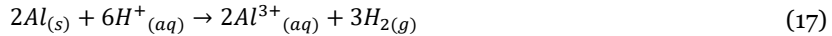
1 M oxalic acid	95 °C	98% Li; 97% Co (precipitated and recovered as CoC ₂ O ₄)	Zeng <i>et al.</i> , 2015
4 M NH ₃ , 1.5 M (NH ₄) ₂ SO ₄ , 0.5 M Na ₂ SO ₃	80 °C	95% Li, 90% Ni, 81% Co, 4.3% Mn	Zheng <i>et al.</i> , 2017
1 M H ₂ SO ₄ , 0.075 M NaHSO ₃	95 °C	97% Li, 92% Co, 96% Ni, 88% Mn	Meshram <i>et al.</i> , 2015
3.5 M HCl, 4.0 M NH ₄ Cl, 0.5 M H ₂ O ₂	80 °C	100% Li, 100% Ni, 95% Co, 100% Mn	Yi <i>et al.</i> , 2021
1.25 M H ₂ SO ₄ , 0.75 g/g NiMH/LCO powder	75 °C	100% Li, Co	Liu, F. <i>et al.</i> , 2019
2.0 M H ₂ SO ₄ , 50 vol-% Kraft black liquor	80 °C	100% Li, 98% Co, 100% Mn, 97% Ni	Carreira <i>et al.</i> , 2024
5 M H ₂ SO ₄ , 10 vol-% methanol	90 °C	99% Li, Co	Kong <i>et al.</i> , 2023
300 g/L glycine, 10% H ₂ O ₂	80 °C	91% Li, 97% Co	Chen <i>et al.</i> , 2021
1/2 molar ratio of Choline chlo- ride/urea	180 °C	95% Li, Co	Wang <i>et al.</i> , 2020
Fe ₂ (SO ₄) ₃ solu- tion (9 g/L Fe ³⁺), bioleaching with Acidithiobacillus ferrooxidans, ul- trasonification	30 °C	67% Li, 19% Co, 50% Mn, 34% Ni	Nazerian <i>et al.</i> , 2022
2 M H ₂ SO ₄ , 1.06 g/L Fe, 1 mol/mol Cu/LCO	30 °C	> 95% Co	Porvali <i>et al.</i> , 2020a
2 M H ₂ SO ₄ , 0.1 g/g black mass coarse frac- tion/black mass fine fraction	80 °C	> 99% Co, Li	Peng <i>et al.</i> , 2019
2 M H ₂ SO ₄ , 28.3 g pure LFP/50 g black mass	60 °C	100% Co, 88% Ni, 91% Mn, 100% Li	Zou <i>et al.</i> , 2024a

2.3.2 Metallic reductants

A considerable portion of the research discussed above has focused on the leaching of cathode materials in isolation, *i.e.*, using pure battery chemicals and reductants. Nevertheless, real-life recycling processes deal with industrial black masses which also contain various other components that can greatly affect the leaching process – as discussed in Section 2.1. From redox reactions point of view, potentially the most interesting of these components are the metallic contents originating from current collectors and casing materials – Cu, Al, and Fe – as these metals can act as reductants toward cathode metal oxides (Equations 7, 11, and 12 in Table 1), as previously demonstrated in studies by Joulié *et al.* (2017), Peng *et al.* (2019), and Ghassa *et al.* (2020). As these metallic components are very often present in industrial black masses (Wilke *et al.*, 2023), their utilization for cathode material dissolution may potentially allow for the development of a leaching process with a significantly lower external reductant demand. Nonetheless, redox reaction facilitation between cathode metal oxides and current collector metals Cu and Al requires a catalyst – an aqueous species or ion pair capable of both oxidation and reduction – such as the Fe²⁺/Fe³⁺ ion pair (Equation 16, Peng *et al.*, 2019; Porvali *et al.*, 2020a), necessitating a sufficiently high solution Fe concentration to allow for efficient electron transfer.

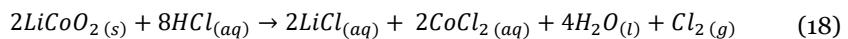


Although Equation 16 only considers Cu, aluminum has also been hypothesized to act via a similar mechanism (Peng *et al.*, 2019). However, Al dissolution in sulfate media has previously been found to be considerably slower when compared with Cu (Chernyaev *et al.*, 2022), and the potential side-reaction of H₂ gas evolution (Equation 17) in combination with the low reactivity of the H₂ molecule (Baade *et al.*, 2001) significantly decreases the Al reductive efficiency.

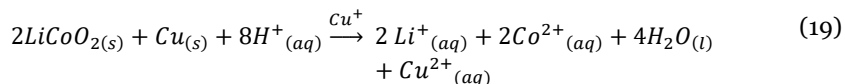


2.3.3 Chloride media

As an alternative to the traditional sulfuric acid lixiviants, some research has also been conducted in hydrochloric acid media, as HCl has been claimed to be a more efficient lixiviant when compared to H₂SO₄, due to the suggested reductive nature of the Cl⁻ ion toward LIB cathode materials (Equation 18; Takacova *et al.*, 2016; Porvali *et al.*, 2019). Although the studies mentioned above did not include any Cl₂ gas measurements to support this claim, this interaction has latterly been suggested by indirect measurements in other studies involving various NMC-type cathode materials (Xuan *et al.*, 2019; Xuan *et al.*, 2021; Yi *et al.*, 2021).



In addition to direct cathode metal oxide reduction, chloride ions can promote cathode material dissolution via the stabilization of cuprous chloride complexes – such as $[\text{CuCl}_2]^-$ – which can catalyze redox reactions between reductant metals and cathode materials (Equation 19) akin to the $\text{Fe}^{2+}/\text{Fe}^{3+}$ ion pair discussed earlier (Equation 16). **N.B.**, in Equation 19, Cu^+ refers to any soluble chloro-complex (Zhao *et al.*, 2013) with Cu in the +1-oxidation state.



The requirement for chloride ions in this system stems from the fact that such a leaching system is not thermodynamically viable in sulfuric acid media due to the Cu^+ ion instability in aqueous and sulfate solutions (Greenwood and Earnshaw, 1997). The use of cuprous chloride complexes has previously been studied extensively in other research fields, particularly in the leaching of copper minerals – such as chalcopyrite (Lundström *et al.*, 2005) and chalcocite (Hashemzadeh *et al.*, 2019) – and gold (Seisko *et al.*, 2019). Nevertheless, in these applications, Cu^+ complexes are merely an intermediate species resulting from oxidative reactions involving Cu^{2+} . Consequently, these systems require an additional oxidant – like oxygen gas – to regenerate copper back to the +2-oxidation state, whereas the reductive system described in Equation 19 uses metallic Cu to reduce Cu^{2+} species back to the +1-state after initial oxidation. On the other hand, due to the high oxidizing tendency of Cu^+ species (Raudsepp and Beattie, 1986), this leaching system may be prone to interferences by atmospheric oxygen, potentially resulting in overconsumption of Cu unless oxygen can be eliminated from the system by, *e.g.*, inert gas purging.

2.3.4 Considerations for solution purification

Metallic elements such as Fe, Cu, and Al have previously been shown to be efficient reductants in hydrometallurgical recycling processes. Nonetheless, any elements entering the process require a dedicated removal step – with associated environmental impacts and technical challenges. Typically, Cu, Fe, and Al are removed from the solution after leaching and before valuable battery metals (Co, Ni, Mn, Li) recovery, which may lead to unwanted losses of these target metals – *e.g.*, by co-precipitation or co-extraction.

Copper is the most noble species present in battery leaching systems, therefore, its removal by cementation, H_2S precipitation, or SX is state-of-the-art technology (Latini *et al.*, 2022). Furthermore, Cu removal does not cause additional challenges for Co or Ni recovery due to its distinct chemical properties. In contrast to copper, iron is typically not recovered as a product but rather precipitated as a hydroxide or other mixed precipitates (Dutrizac and Monhemius, 1986). Fe can be precipitated either individually or together with Al, although significant amounts of battery metals may be lost within these precipitates –

losses of up to 4–5% of Li, Ni, and Co have been reported in previous literature (Chernyaev *et al.*, 2023; Zou *et al.*, 2024b).

Moreover, Al is not a favorable element in PLS due to the lack of industrially viable methods able to recover the element as a valuable product from aqueous solutions (Sristava and Meshram, 2023). Therefore, in downstream processes, Al is typically precipitated and discarded as $\text{Al}(\text{OH})_3$, which can cause problems in the subsequent filtration step due to the colloidal nature and gel-like properties of this precipitate (Zhang *et al.*, 2022). In addition to the poor filterability characteristics, $\text{Al}(\text{OH})_3$ precipitation has been reported to result in notable valuable battery metal losses as co-precipitates. For example, Wang and Friedrich (2015) reported losses of 3–5% for Co, Ni, and Mn, whereas Chernyaev *et al.*, (2021) reported losses of up to 10% Ni, 2% Co, and 10% Li to the hydroxide cake. Due to these drawbacks related to Al hydroxide precipitation, alternative methods like phosphate precipitation have been studied (Alemrajabi *et al.*, 2022; Chernyaev *et al.*, 2023) with promising results related to filterability characteristics and co-precipitation.

If chloride-rich processes are used in battery leaching, copper may instead be precipitated as atacamite ($\text{Cu}_2\text{Cl}(\text{OH})_3$) (Lundström *et al.*, 2016), whereas Fe and Al can be precipitated as their respective hydroxides by pH increase. In addition to solution purification, the presence of a high concentration of Cl^- ions may necessitate different approaches with respect to valuable metals recovery – *e.g.*, by the choice of different solvent extraction chemicals when compared with sulfate media (Torkaman *et al.*, 2017).

2.3.5 Implications of previous literature for the current work

Previous literature shows that lithium-ion batteries comprise multiple chemically different components – such as cathode and anode materials, electrolyte, and separator – which must be considered as a part of recycling. Upon reaching EoL, batteries should primarily be directed for use in a secondary application, *e.g.*, as stationary energy storage units. Only when batteries can no longer be used, should they be recycled to recover their valuable materials.

The first stage of hydrometallurgical battery recycling – *i.e.*, leaching – is electrochemical in nature. Current literature commonly reports final metal extractions to solution, however, the electrochemical phenomena in the system – and therefore, the current efficiencies of the associated reduction reactions – are often overlooked. Moreover, the complexation and stability of soluble species can have significant impacts on the predominant reactions. Consequently, this work investigates the prevalent electrochemical reactions in battery leaching systems and the current efficiencies related to these processes.

Industrial black mass is not homogeneous by nature, but varies based on the constituent battery types and pre-treatments used for preparation. For example, the Ni content in EV batteries has substantially increased in recent years, which will result in a waste with a very high Ni content and low Co and Mn contents as these batteries reach their EoL. On the other hand, the content of metallic fractions (Fe, Cu, Al) is more dependent on the pre-treatment methods applied in preparation for metallurgical recycling. The complexity and variance between

different black masses poses challenges for a comprehensive analysis of chemical reactions within black mass leaching systems. Therefore, careful selection of industrial raw materials has been performed in this work, with the aim of having a low initial content of Fe or current collector metals in studies investigating additions of these materials. Such careful raw material selection also allows for a statistical analysis of the leaching results – an approach rarely undertaken in existing literature.

3. Experimental

3.1 Materials and Equipment

Leaching experiments detailed in Publications I–IV and Compendium were all conducted in sulfuric acid-based lixivants using H_2SO_4 (95–97%) to prepare leaching solutions of different concentrations. Additionally, Publication I and some experiments in Publication II – as well as the individual Compendium experiment – added NaCl ($\geq 98\%$) to the lixivants to investigate the impacts of chlorides on LIB leaching performance. Publication I also used HCl (37%) for this purpose in selected experiments. All the chemicals mentioned above were provided by VWR Chemicals, Belgium. Additionally, all solutions were prepared using deionized water (15 $\text{M}\Omega\cdot\text{cm}$, Merck Elix Essential 15, Germany).

Regarding the LIB materials investigated, Publications I and II used commercial virgin LIB cathode powders (NMC₁₁₁, $> 99.5\%$, MSE Supplies, USA, in Publication I; LiCoO_2 , $> 99.5\%$, Alfa Aesar, Germany, in Publication II) in leaching experiments, whereas Publications III and IV – and the individual Compendium experiment – used industrially produced black mass instead. The industrial black mass used in Publication III originated mainly from LCO-type mobile phone and laptop batteries, whereas the black mass used in Publication IV and the Compendium experiment originated primarily from NMC₁₁₁-type EV batteries. Both black mass types were produced by an industrial battery recycling company via a process entailing two-step crushing and magnetic separation (Pudas *et al.*, 2015). The black masses were obtained as sieved fractions with a particle size of < 2 mm (Publication III) and < 1 mm (Publication IV and Compendium). The black mass used in Publication III was further sieved down to < 500 μm with a vibratory sieve (Fritsch Analysette 3, Idar-Oberstein, Germany) prior to experiments to reduce the current collector content in the black mass and allow for a more precise investigation of reductant addition effects on the leaching performance.

Other chemicals used in leaching experiments included copper powder (99.5% Cu, Sigma-Aldrich, USA) in Publication II, ferric sulfate ($\text{Fe}_2(\text{SO}_4)_3 \cdot n\text{H}_2\text{O}$, VWR chemicals, Belgium) in Publication III, and ferrous sulfate ($\text{FeSO}_4 \cdot 7\text{H}_2\text{O}$, $\geq 99.0\%$, Sigma-Aldrich, USA), LiFePO_4 cathode powder ($> 98\%$, MSE Chemicals, USA), and hydrogen peroxide solution (50% H_2O_2 , Sigma-Aldrich, USA) in Publication IV. Additionally, Publication III used Cu and Al current collector foils originating from LIB production scrap, whereas Publication IV used reclaimed copper from an industrial battery recycling process. The Cu and Al materials

were processed with a cutting mill (Retsch SM 300, Germany) to shred them to ~1 mm flakes to ensure a more consistent particle size of the materials.

Leaching experiments were performed using several different setups. In experiments using pure commercial cathode chemicals, a smaller, 500 mL reactor was used. This was done to avoid the extensive use of virgin cathode chemicals. Publication II used a 500 mL round-bottom jacketed glass reactor with a circulating water bath (Lauda A100 Germany). This setup was utilized to resemble the setup previously used by Porvali *et al.* (2020) for a maximum comparability between results reported in their study and Publication II. Publication I used a 500 mL single-walled glass reactor heated with a submersible water bath (Lauda AQUAline AL 25, Germany) to resemble the reactor system used by Porvali *et al.* (2019), albeit using a smaller reactor and lower S/L ratios.

In experiments using industrial battery waste (Publications III and IV and Compendium), a larger, 1000 mL flat-bottomed jacketed glass reactor was used in conjunction with a circulating water bath (Haake 1, Thermo Electronics, Germany). In these experiments, a larger reactor volume was deliberately chosen when compared with experiments dealing with pure cathode chemicals and low S/L ratios to allow for extra space within the reactor and thereby account for potential frothing associated with the leaching of industrial black mass. In all publications, agitation was achieved using an overhead stirrer (VWR VOS 16) and a stirrer shaft with a 45° angled four-blade polytetrafluoroethylene (PTFE) impeller with a diameter of 50 mm – in conjunction with 500 mL reactors (Publications I and II) – or 90 mm in the case of 1000 mL reactor volume (Publications III and IV, Compendium).

In all publications, solution samples were taken during leaching with a silicone tube attached to a syringe and immediately filtered using syringe filters (0.45 µm polyethersulfone, VWR, USA, Publications I and II) or filter papers (grade 005, Ahlstrom-Munksjö, Finland, Publication III; Grade 41, Whatman, UK, Publication IV and Compendium). The samples were subsequently diluted with 2% HNO₃ solution (prepared from 65% HNO₃, VWR Chemicals, Belgium) and analyzed with atomic absorption spectrometry (AAS; Thermo Scientific, iCE 3000, USA). In Publication IV, ICP-OES (inductively coupled plasma–optical emission spectrometry; Agilent 5900 SVDV, USA) was additionally used to analyze solution Al concentrations. Leaching yields were calculated using Equation 20 which considers the effects of sampling and evaporation.

$$Y = \frac{c \cdot (V_i - V_{sc} - V_e \cdot \frac{t_x}{t_f}) + m_{xc}}{m_i} \cdot 100\% \quad (20)$$

where Y = leaching yield
 c = solution metal concentration at sampling interval x (g/L)
 V_i = initial volume (mL)
 V_{sc} = cumulative sample volume prior to sampling interval x (mL)
 V_e = total volume lost upon evaporation (mL)
 t_x = time at sampling interval x (min)
 t_f = total leaching time (min)

m_{xc} = cumulative metal losses upon sampling prior to sampling interval x (g)

m_i = initial mass of metal in the feed (g)

Furthermore, the evaporated solution volume (V_e) and metal losses upon sampling at each sampling interval (m_x) were calculated with Equations 21 and 22.

$$V_e = V_i - V_f - V_{s\ tot} \quad (21)$$

where V_f = final solution volume after experiment (mL)

$V_{s\ tot}$ = total volume of samples during experiment (mL)

$$m_x = c \cdot V_s \quad (22)$$

where V_s = sample volume at timepoint x (mL)

In all publications, leaching progress was additionally monitored with redox potential measurements. In Publications II, III, and IV, this was undertaken with a Ag/AgCl vs. Pt redox probe (Mettler Toledo InLab, USA), whereas Publication I used a calomel reference electrode (SCE, B521, SI Analytics, Germany) in combination with platinum wire (Kultakeskus Oy, Finland) instead – to allow for the use of a salt bridge between the electrode probe and leach solution and thereby avoid damaging the probe when measuring high-temperature solutions ($T \geq 70$ °C). In Publication I, the leaching process was also monitored by Cl_2 gas measurements using a hand-held single-gas detector (WatchGas UNI mp100, 0.1–50 ppm Cl_2 , the Netherlands), whereas Publication III followed the leaching progress by titration of the residual acid from solution samples. The titration was done by diluting a part of a sample with 50–80 mL of deionized water and reacting the solution with a few crystals of $\text{Na}_2\text{S}_2\text{O}_3 \cdot 5\text{H}_2\text{O}$ (99.8%, VWR, Belgium) – to reduce any soluble iron to the Fe^{2+} state, thereby preventing unwanted ferric iron precipitation – after which the solution was titrated with 0.1 M NaOH solution (Merck, Germany) to determine the H_2SO_4 concentration. Methyl orange solution was used as the indicator, prepared from solid powder (Schering A.G Berlin, Germany) and deionized water.

In Publications I–III, raw material and leach residue mineral compositions were determined with X-ray diffraction (XRD; PANalytical X'Pert Powder – the Netherlands – with Cu K α radiation source operated at 40 mA current and 40 kV voltage), using Rietveld refining (HighScore PLUS, The Netherlands) to refine and assess the obtained diffractograms. In Publication III, solid samples were also analyzed with scanning electron microscopy in combination with energy dispersive X-ray spectroscopy (SEM-EDX; Tescan Mira³, Czech Republic) to obtain micrographs of solid particles for surface investigation.

3.2 Raw material characterization

In order to calculate leaching yields from measured solution metal concentrations, chemical compositions of the black masses used in Publications III and IV were analyzed. This analysis was done by digesting four small samples (5 g each) of the respective black masses in aqua regia (1:3 molar ratio of HNO₃/HCl) under a boiling temperature for 30 minutes. Samples of the resulting solutions were then diluted with 2% HNO₃ solution and analyzed with AAS and ICP-OES for their metal concentrations (Table 3). Additionally, the black mass F⁻ content in Publication III was determined using a fusion method (performed by ALS Finland Oy), where the sample was fused with a carbonate flux and dissolved in a pH-buffered citric acid solution, followed by fluoride-ion content measurement with an ion-selective electrode. For comparison between industrial black masses and pure chemicals, Table 3 also shows a typical chemical composition of pure NMC111-type cathode powder.

Table 3. Chemical compositions of black masses used in Publications III and IV and a typical NMC111-type cathode powder (MSE Supplies, 2024), reported in wt-%. < 2 mm refers to black mass before further sieving. Black mass compositions are adopted from Publications III and IV, © 2021, © 2024 The authors, reproduced from Elsevier under CC BY 4.0.

Material	Li	Ni	Mn	Co	Al	Fe	Cu	F
Publication III black mass								
< 2 mm	3.7	2.3	2.6	26	3.4	0.6	4.0	3.4
> 500 μm	2.7	2.2	2.0	19	16	1.1	13	n/a
< 500 μm	3.8	2.5	2.8	26	2.3	0.5	1.5	n/a
Publication IV black mass								
< 1 mm, Average	3.3	8.8	7.9	10	3.5	0.1	7.5	n/a
Standard deviation	0.08	0.36	0.21	0.55	0.18	0.02	1.35	n/a
Pure cathode powder								
NMC111	7.6	20.2	16.0	20.3	n/a	0.0025	0.001	n/a

As can be calculated from concentrations shown in Table 1, metals typically only account for around 40–55% of the total black mass weight. In comparison, pure NMC cathode material is composed of ~65% cathode metals Li, Ni, Mn, and Co, whereas the rest (~35%) is mainly oxygen bound to the molecular lattice. Using the same ratio between cathode metals and oxygen, the mass accounted for by oxygen in black masses is around 14–19%, and the remaining fraction not related to either metals or oxygen (26–46%) is mostly plastic fragments and graphite.

In addition to black mass samples, the reclaimed copper scrap used as reductant in Publication IV was also analyzed by total dissolution in aqua regia followed by solution analysis by ICP-OES to ascertain that no unwanted impurities would be introduced upon addition to the solution. The scrap was found to be ~99.5% pure Cu.

3.3 Leaching experiments

In terms of research objectives, the publications were divided into two categories. Publications I and II studied the fundamental leaching phenomena occurring during LIB cathode material leaching in the absence of other black mass components. For this purpose, these experiments used low solid/liquid (S/L) ratios – between 17 g/L (Publication I) and 28 g/L (Publication II) – to keep acid consumption low during experiments. In contrast, Publications III and IV studied leaching of industrially produced black mass, and therefore, a high S/L ratio of 200 g/L – relevant to industrial leaching processes – was used. All experimental procedures are presented in more detail in their respective Publications I–IV.

For all experiments, the lixiviant solution was preheated to the desired temperature before any cathode material or black mass additions. Publications II and III used a single temperature throughout the experiments – 30 °C in Publication II, 60 °C in Publication III – whereas Publications I and IV studied a range of leaching temperatures – 30–80 °C in Publication I, 30–70 °C in Publication IV. In Publication III, metallic reductants were added after 30 minutes of leaching, whereas in other publications, any solid additives – such as metallic Cu – were added into the leaching reactor at the start of the experiments, along with LIB cathode powder or black mass. In experiments studying H₂O₂ as a reductant (Publication IV), the peroxide solution was steadily added throughout the first hour to avoid excessive O₂ gas formation and minimize the potential risk of violent froth formation and subsequent reactor overflow.

Publication II studied the effects of solution chloride-ion concentration with the goal of stabilizing various chloro-complexes of the Cu⁺ ion to act as catalysts for cathode material reduction by metallic copper (Equation 19) and subsequently enhance cathode material leaching. The study used 0.5 and 1.0 M H₂SO₄ as the base lixiviants, the chloride concentration of which was adjusted with NaCl – dissolved into the solution before each experiment – to obtain Cl⁻ concentrations between 0.1–3.2 M. In these experiments, the reactor was also purged with nitrogen gas (99.99% N₂, Linde, Finland) at a flow rate of 0.5 L/min, regulated with a rotameter (LH-ZC51-HR, Kytola, Finland). Nitrogen purging was started 10 minutes before the commencement of each experiment and continued throughout the leaching time to prevent atmospheric oxygen from affecting the leaching system. Such gas purging was not used in any other of the publications.

Publication I investigated the reactions involved in the leaching process of a pure NMC111-type cathode powder in sulfate, chloride, and mixed sulfate–chloride solutions. For this purpose, the study used H₂SO₄, HCl, and H₂SO₄–NaCl solutions – all in the concentration of 1 M. Leaching phenomena were additionally monitored with a redox probe and chlorine gas detector (WatchGas UNI mp100, 0.1–50 ppm Cl₂, the Netherlands).

Lastly, both Publications III and IV studied the effects of various parameters on industrially produced black mass leaching in sulfuric acid solutions. For this purpose, both publications used 2 M H₂SO₄ exclusively as the leaching medium, with various reductants added to improve cathode metal oxide dissolution.

3.4 Kinetic studies and regression analysis

In addition to the comparison of leaching yield results between experiments, Publications II, III, and IV used further mathematical analysis methods to allow for more rigorous conclusions to be made. Publication II studied the kinetics of the investigated leaching reaction to enable a more precise comparison to earlier studies. For this purpose, the reaction was assumed to conform to a shrinking particle model, with chemical reaction rate as the controlling factor (Equation 23). The following considerations with respect to the model chosen in the study were made based on Levenspiel (1999, pp 568–579). A shrinking-core model was chosen, as such an approach is typically more representative when compared to progressive-conversion models. The special case for shrinking spherical particles – as opposed to a particle with a shrinking core – was applied, as particle dissolution was assumed to occur without the formation of a solid reaction product layer at the particle surface. Lastly, agitation was deemed to be sufficient as to eliminate film diffusion resistances, leading to the conclusion of a chemical-rate controlled model as the most representative of reality – as opposed to a film diffusion-controlled model. **N.B.**, although a shrinking particle model was chosen in this work, the mathematical representation for a chemical reaction-controlled shrinking-core model – assuming the formation of a solid reaction product layer – is identical. Furthermore, the use of the same model as applied by Porvali et al. (2020) allowed for a direct comparison between their findings and the results obtained in Publication II.

$$\frac{t}{\tau} = 1 - (1 - x)^{\frac{1}{3}} \quad (23)$$

Where t = time (min)
 τ = time required for complete conversion (min)
 x = dissolved fraction of the studied element

To allow for reaction rate interpretation with trendline fitting, Equation 23 was modified by substituting the inverse of reaction rate constant, $1/k_c$ for τ to obtain Equation 24.

$$k_c \cdot t = 1 - (1 - x)^{\frac{1}{3}} \quad (24)$$

Where k_c = rate constant (min^{-1})

Publications III and IV used a DoE (Design of Experiments) methodology in conjunction with regression modeling to assess the statistical effects of different parameters on the black mass leaching process. DoE is a statistical tool designed to allow for the assessment of interaction effects between multiple studied variables, in contrast to the often used one-factor-at-a-time (OFAT) design which only allows for the evaluation of variable effects individually (Shina, 2022). In Publications III and IV, DoE was used in combination with regression modeling to create leaching models able to predict cathode metal yields based on chosen

experimental variables. The experimental designs were selected using two versions of the software MODDE (Sartorius, Germany). Publication III (MODDE 8) used a central composite face-centered (CCF) design with two factors – Cu and Al additions. This model design was chosen due to the advantages of central composite designs which include easy fitting, small number of required experiments, reasonably high efficiency, and the possibility for sequential experimentation – allowing for an expansion from a two-level factorial design by the addition of axial points and additional center points (Gilmour, 2010). On the other hand, Publication IV (using MODDE 13) used a full-factorial design with four factors – temperature, solution Fe concentration, and additions of Cu and H₂O₂. Such a full-factorial design was chosen to test for each parameter and combination individually, thereby yielding the highest amount of data, which was deemed necessary due to the inhomogeneity of the raw material. Both models were fitted using the partial least squares method (Wold *et al.*, 2001).

4. Results and discussion

This section presents and discusses the main results reported in Publications I–IV. It is divided into two subsections so that Section 4.1 focuses on leaching systems using pure LIB cathode powders with the goal of providing a better understanding of the impacts that individual elements and process conditions can have on pure LIB leaching systems, whereas Section 4.2 deals with leaching phenomena associated with industrially produced impure LIB black mass.

Section 4.1 discusses the results of Publication I which investigated various fundamental leaching phenomena occurring during pure LIB cathode material leaching in sulfate and chloride-based media without added reductants, specifically focusing on interactions between NMC₁₁₁ cathode powder and soluble Mn²⁺ and Cl⁻ ions. The section proceeds with the topic of cathode material leaching in the presence of chlorides (Publication II), with the addition of a new reductive component into the system in the form of metallic Cu powder – representing a typical current collector material used in LIBs. Copper acts as a reductant toward cathode metal oxides (Equation 19), enabled by the complexation with chloride ions. This leaching system was studied under a wide range of chloride concentrations (0.1–3.2 M NaCl).

In contrast, section 4.2 discusses the performance of current collector foils – contained within the studied industrially produced black masses – as reductants toward LIB cathode materials. The performance is evaluated using data from both kinetic experiments and regression modeling. These results are supplemented with a brief CO₂ footprint comparison between different reductants – Cu, Al, and H₂O₂ – along with observations of a black mass leaching experiment performed using a chloride-containing lixiviant.

4.1 Leaching of pure Li-ion battery cathode powders

Publications I and II studied the leaching of pure LIB cathode powders to investigate the leaching phenomena in selected leaching environments. Leaching was studied in both sulfate and chloride media (Publication I). In addition, a wide range of chloride concentrations were investigated to study the reductive capabilities of soluble Cu⁺ complex species toward LIB cathode material (Publication II).

4.1.1 Leaching in sulfate and chloride solutions

The research in Publication I focused on identifying the main dissolution phenomena and redox reactions that occur during LIB cathode material leaching in lixiviants based on sulfates, chlorides, and their mixtures. The goal was to investigate the leaching mechanisms and spontaneous redox reactions taking place in LIB leaching systems in the absence of external reductants, *i.e.*, reducing agents like hydrogen peroxide.

As discussed in Section 2.3, a part of the LIB cathode material can be leached in acidic solutions without any added reductants. Nonetheless, some researchers have used HCl as the lixiviant instead of H₂SO₄, based on the supposed reductive properties of the Cl⁻ ion toward LIB cathode metal oxides (Takacova *et al.*, 2016; Porvali *et al.*, 2019). This hypothesized reductive property was one of the main motivations behind the research conducted in Publication I. Experiments were initially conducted in H₂SO₄ solutions at temperatures between 30 and 80 °C to establish reference points against which results obtained using chloride-containing media could be compared. In addition to moderate (~40%) transition metals dissolution in sulfuric acid media (Figure 5b), it was found that at temperatures of $T \geq 50$ °C, Mn started to precipitate out of the solution (Figure 5). This precipitation was additionally accompanied by a slight increase in other battery metal yields at 80 °C.

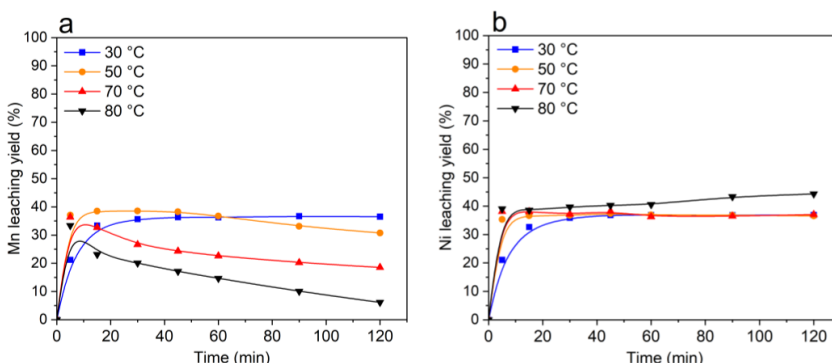


Figure 5. Leaching yields of a) Mn and b) Ni in 1 M H₂SO₄ solution. Adapted from Publication I, © 2023 The authors, reproduced from Elsevier under CC BY 4.0.

The precipitated manganese compounds were identified from leach residues with XRD as a birnessite-type lithium–manganese oxide – Li₄Mn₁₄O₂₇·xH₂O – and manganese dioxide, MnO₂ (Figure 6). In addition, the cathode material lithium content in the leach residue was found to decrease in response to increased reaction temperatures – from the pristine LiNi_{1/3}Mn_{1/3}Co_{1/3}O₂ (in the pure chemical) to Li_{0.4}Ni_{1/3}Mn_{1/3}Co_{1/3}O₂ (at $T = 30$ °C) and to Li_{0.24}Ni_{1/3}Mn_{1/3}Co_{1/3}O₂ (at $T = 50$ °C). Furthermore, after leaching at $T = 80$ °C, a completely delithiated phase – Ni_{0.33}Mn_{0.33}Co_{0.33}O(OH) – was identified as well. Similar findings with respect to delithiation and manganese precipitation have previously been reported by Billy *et al.*, (2018), albeit at a lower temperature and with longer reaction times.

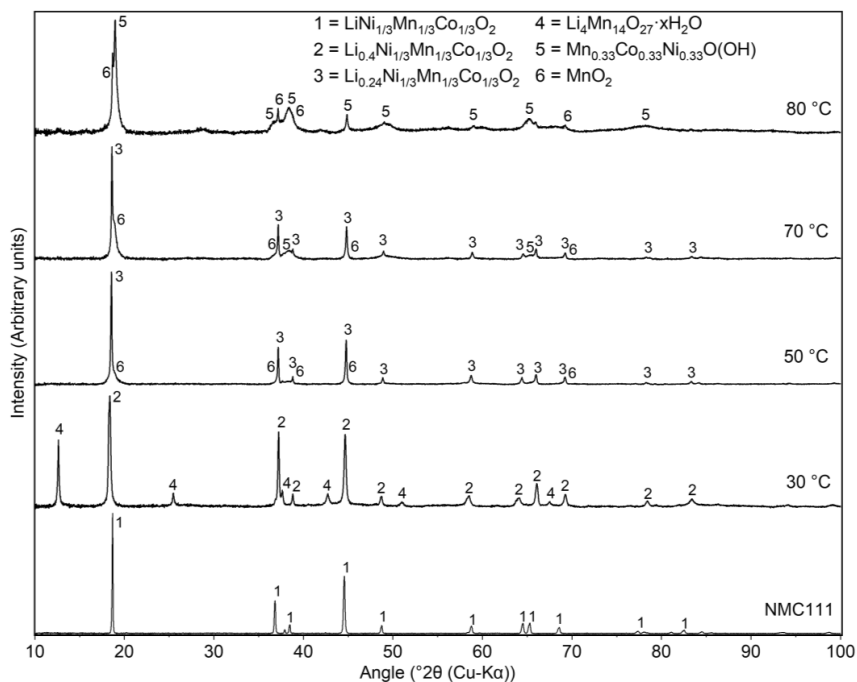
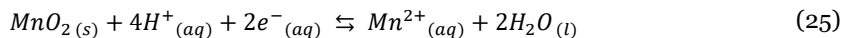
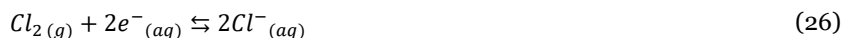


Figure 6. XRD diffractograms of pure NMC111 powder and leach residues after leaching in 1 M H_2SO_4 solution at different temperatures. Adopted from Publication I, © 2023 The authors, reproduced from Elsevier under CC BY 4.0.

Soluble manganese has previously been suggested to act as a reductant toward the NMC111 cathode material by the oxidation of Mn^{2+} ions to the 4+-state (Kim *et al.*, 2022; Equation 25). This reaction has a very high reduction potential – $E = 1.20\text{--}1.23$ V vs. SHE between 30 °C and 80 °C (HSC 9.4.1, Metso, Finland) – and is therefore suggested to be a thermodynamically viable reductant in a pure system for NMC-type cathode materials with a very high oxidative power.

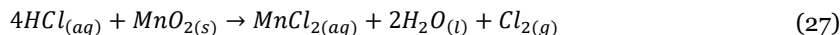


When comparing leaching phenomena in 1 M HCl and 1 M $\text{H}_2\text{SO}_4\text{--NaCl}$ solutions, almost equivalent leaching yields were measured for Co, Ni, and Li. However, manganese behavior changed significantly – in the presence of chlorides, no extensive Mn precipitation was observed. This was attributed to Cl^- ions acting as the reductant (Equation 26) in preference to Mn^{2+} ions (Equation 25).



Nevertheless, the theoretical reduction potential of this reaction (Equation 26) is even higher than that of Equation 25 (1.29 V at 80 °C, HSC 9.4.1), and should therefore be thermodynamically less favorable. However, the relationship between the two reactions is known to be heavily dependent on solution pH (Hao

et al., 1991; Li *et al.*, 2019), with chlorine gas evolution being particularly favored at pH levels below 1, *i.e.*, at acid concentrations above 0.1 M (Tu, 1993) – as was the case in these experiments. This property has also been used historically to generate Cl₂ gas for textile bleaching via the Weldon process (Equation 27; Pisarczyk, 2005; Schmittinger *et al.*, 2011).



The redox potentials measured during leaching in H₂SO₄ and HCl solutions (Figure 7) are in line with the observations described above, as the experiments exhibit sufficiently high potentials to allow for both Mn²⁺ and Cl⁻ oxidation reactions to occur. Interestingly, the presence of chlorides appears to limit the measured redox potentials to around 1300 mV vs. SHE – which corresponds to the Cl₂ evolution potential – possibly due to the redox electrode ability to only measure the potential of the active Cl₂ formation reaction rather than the entire system.

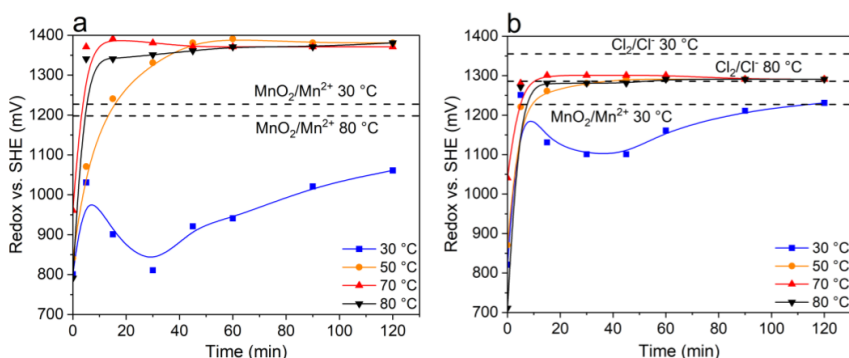


Figure 7. Redox potentials measured during NMC111 leaching experiments in a) 1 M H₂SO₄, b) 1 M HCl. The dashed lines indicate the theoretical reduction potentials of the MnO₂/Mn²⁺ and Cl₂/Cl⁻ reactions at 30 and 80 °C. Adapted from Publication 1, © 2023 The authors, reproduced from Elsevier under CC BY 4.0.

Furthermore, the prevalence of chlorine gas evolution as the anodic reaction was also confirmed by Cl₂ gas measurements, as both HCl and H₂SO₄–NaCl solutions were found to generate notable amounts of Cl₂ (≥ 50 ppm) during NMC111 cathode powder leaching at elevated temperatures ($T \geq 50$ °C; Figure 8). Between the two chloride-containing media, Cl₂ gas evolution was markedly higher in mixed H₂SO₄–NaCl media – with also higher associated Ni yields (Figure 9) – when compared with HCl alone. Also, Mn and Co had a similar leaching behavior when compared with Ni. Although the measured Cl₂ concentrations between the two lixivants were very similar (Figure 8), the gas detector reading reached its maximum display value considerably faster in experiments using H₂SO₄–NaCl media. These pronounced effects in the presence of NaCl were hypothesized to be caused by an increased Cl⁻ ion activity associated with chloride salts in comparison to HCl (Puvvada *et al.*, 2003).

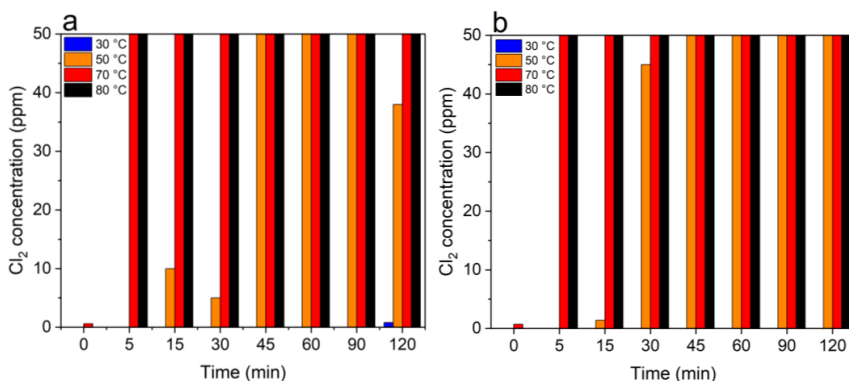


Figure 8. Measured Cl_2 gas concentrations evolved during NMC111 leaching experiments in a) 1M HCl, b) 1M H_2SO_4 -NaCl. Adapted from Publication I, © 2023 The authors, reproduced from Elsevier under CC BY 4.0.

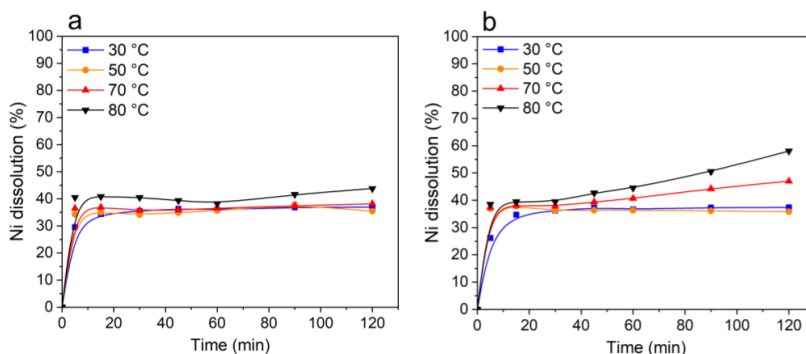


Figure 9. Leaching yields of Ni in a) 1 M HCl, b) 1 M H_2SO_4 -NaCl solution. Adapted from Publication I, © 2023 The authors, reproduced from Elsevier under CC BY 4.0.

Despite the differences in leaching behavior between lixiviants at higher temperatures ($T \geq 50$ °C), all studied leaching systems resulted in almost identical outcomes at a lower temperature ($T = 30$ °C), with virtually no detectable Cl_2 gas evolution or decrease in Mn yield. This suggests that the reduction reactions of Cl^- or Mn^{2+} ions require elevated temperatures to allow for sufficiently high reaction kinetics, or alternatively, a very long reaction time as demonstrated by the results of Billy *et al.* (2018). Nonetheless, the reaction kinetics may also be strongly related to the cathode material composition, as reported earlier by Xuan *et al.* (2019, 2021).

To summarize, the results outlined here showed that Cl^- ions can act as a reductant toward NMC-type cathode materials in pure leaching systems, whereas Mn^{2+} ions can exhibit a similar reductive behavior in sulfuric acid media, resulting in the precipitation as MnO_2 and $\text{Li}_4\text{Mn}_{14}\text{O}_{27} \cdot x\text{H}_2\text{O}$. Both these reactions take place preferentially at elevated temperatures ($T \geq 50$ °C) and require a high oxidative potential ($E \geq 1300$ mV vs. SHE) to occur and are therefore less likely in industrial multimetal black mass leaching systems where alternative reductants – such as Cu, Al, and Fe – are typically present.

4.1.2 Cu as a reductant in the presence of chlorides

Similarly to Publication I, Publication II studied LIB cathode powder leaching in the presence of chlorides, however, using metallic copper powder as an externally added reductant. The study used chloride-containing sulfuric acid solutions to stabilize complexes of Cu^+ species, thereby facilitating redox reactions between LCO-type cathode powder and metallic Cu (Equation 19, Section 2). The main goal was to investigate, whether a previously studied leaching system – using Cu as a reductant and $\text{Fe}^{2+}/\text{Fe}^{3+}$ ion pair as a catalyst (Porvali *et al.*, 2020a; Porvali *et al.*, 2020b) – could be modified to substitute Cu^+ species for the $\text{Fe}^{2+}/\text{Fe}^{3+}$ ion pair, removing the requirement of iron as a catalyst in this process. Leaching experiments with pure LCO cathode material were performed using sulfuric acid as the base lixiviant, the chloride content of which was adjusted with NaCl, as detailed in Section 3.3.

The results showed the investigated leaching system to be viable, with notable Co yields achieved with a Cl^- concentration of 0.1 M (Figure 10). Furthermore, 90% Co yield was also achieved under relatively mild conditions ($T = 30\text{ }^\circ\text{C}$, $[\text{H}_2\text{SO}_4] = 1\text{ M}$, $[\text{NaCl}] = 0.2\text{ M}$) after 2 hours of leaching. Additional analysis also revealed the reaction rate to be comparable with previous results obtained using the $\text{Fe}^{2+}/\text{Fe}^{3+}$ ion pair as the catalyst (reaction rate constant $k = 4.6 \cdot 10^{-3}\text{ min}^{-1}$; Porvali *et al.*, 2020a).

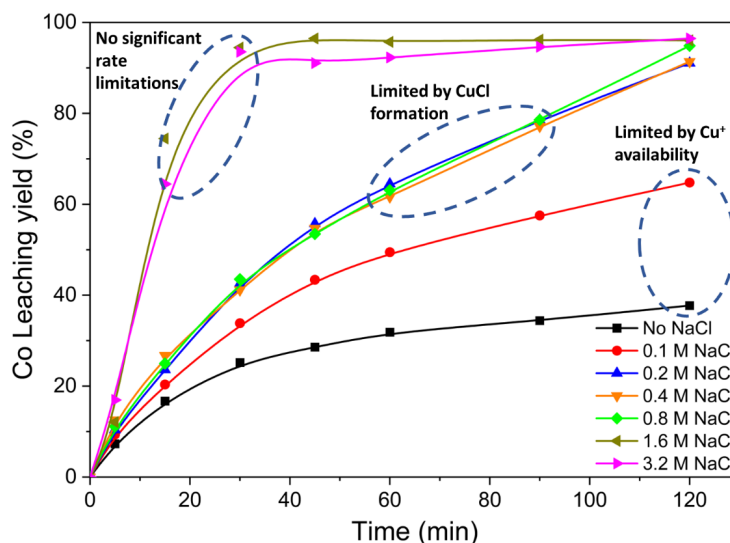
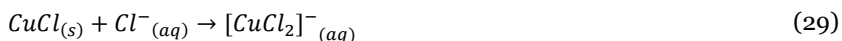
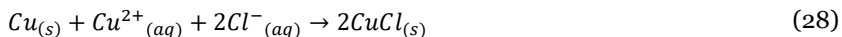


Figure 10. Co leaching yields as a function of time in 1 M H_2SO_4 solution at solution chloride concentrations of 0–3.2 M at 30 °C. Adapted from Publication II, © 2022 The authors, reproduced from Elsevier under CC BY 4.0.

Nevertheless, further increases in chloride concentration up to 0.8 M did not result in improved leaching yields, as the leaching kinetics were observed to plateau. This leaching rate stagnation was hypothesized to be caused by an intermediate reaction involving CuCl precipitation and redissolution (Equations 28 and 29), as evidenced by the formation of visible clusters on copper powder

surfaces, especially with solution chloride concentrations between 0.2 and 0.8 M.



This CuCl layer was proposed to inhibit charge transfer – and consequently, redox reactions – between Cu and LCO, resulting in leaching rate stagnation. The clusters were subsequently identified as CuCl via leach residue XRD analyses (Figure 11). The diffractograms also indicated the presence of a delithiated LCO phase – $\text{Li}_{0.51}\text{CoO}_2$ – which suggests that LCO dissolution undergoes a similar delithiation phenomenon as NMC111 during its dissolution process, as discussed in the previous section and previously reported in literature (Takacova *et al.*, 2016).

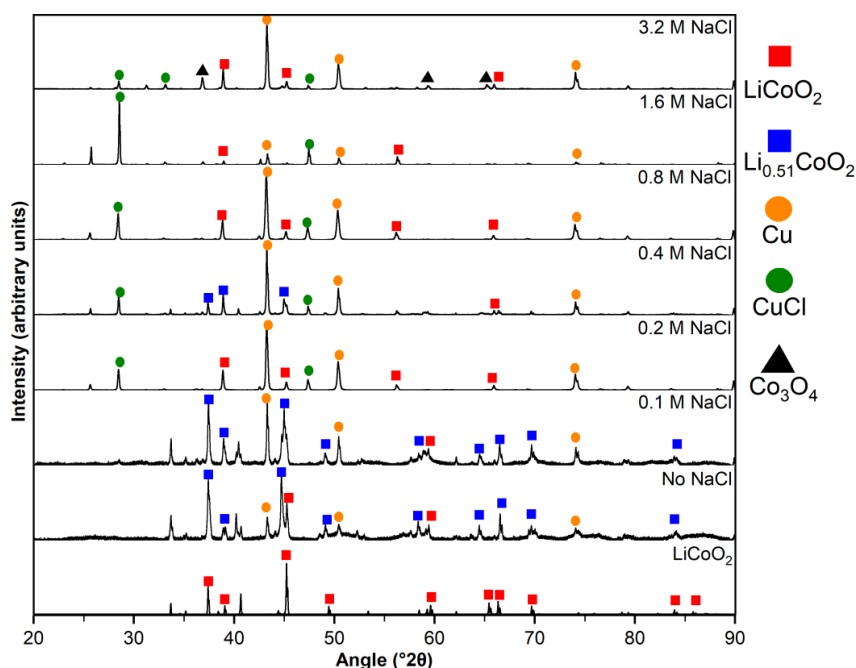


Figure 11. XRD diffractograms of pure LiCoO_2 powder and leach residues after 2 hours of leaching in 1 M H_2SO_4 under various solution Cl^- concentrations. Adopted from Publication II, © 2022 The authors, reproduced from Elsevier under CC BY 4.0.

These results related to CuCl precipitation were also in line with the previous findings of Herreros *et al.* (2005), who reported inhibited dissolution rates at solution molar ratios of $\text{Cl}^-/\text{Cu}^{2+} \leq 8$ because of CuCl precipitation on metallic Cu particle surfaces. Based on the Cu amount used in the experiments of Publication II (0.07 mol Cu, 400 mL lixiviant), this ratio predicts that CuCl formation would be prevented at solution Cl^- concentrations above 1.4 M – a hypothesis

also supported by the calculations of Fritz (1982). Results obtained under solution chloride concentrations of $[Cl^-] \geq 1.6$ M correlated with this prediction, as the dissolution rate of LCO drastically increased under such high chloride concentrations – suggesting an uninhibited reduction by soluble Cu^+ species. Nonetheless, traces of solid CuCl were also found within the leach residues in these experiments (Figure 11), although evidently the formation did not inhibit Cu dissolution and subsequent LCO leaching reactions. It is also possible that the CuCl formation in these experiments occurred after leaching, *e.g.*, as a response to the diminished solution chloride concentration during water washing of the leach residue after filtration.

4.2 Leaching of industrially produced black mass

While Publications I and II studied the leaching of pure LIB cathode powders, Publications III and IV investigated a topic more applicable to real-life processes – leaching of industrially produced black mass. These studies were performed to obtain a deeper understanding on how different reductants affect the leaching process in a more complex system, and in particular, to find new ways to utilize the reductive power of metallic fractions found within black masses as a more environmentally benign alternative to the predominately used H_2O_2 . These studies exclusively used H_2SO_4 as the lixiviant due to its wide-spread application in industrial leaching processes.

4.2.1 Leaching experiments

Publications III and IV studied the utilization of current collector metals Cu and Al as reductants in black mass leaching, however, from different perspectives. Publication III investigated the reductive effects of added Cu and Al scrap on a black mass fraction low on these metals, whereas Publication IV aimed to utilize the Cu and Al content – already present in an iron-lean black mass – supported by temperature increases and iron additions.

At the start of each experiment in Publication III, black mass was first leached without external reductants for 30 minutes to allow any metallic particles contained within to be consumed before controlled reductant additions – thereby ensuring that any subsequent increases in cathode metal leaching yields were specifically a result of the reductants added manually. XRD characterization of the leach residue showed the cathode material dissolution to proceed in a similar manner when compared with pure LCO powder in Publication II, as delithiated LCO was identified from the diffractogram (Figure 12).

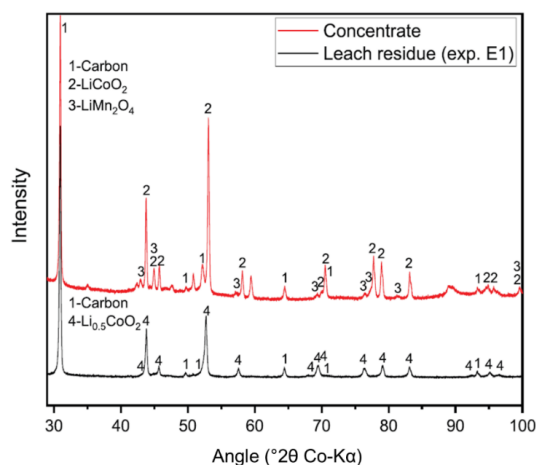


Figure 12. XRD diffractograms of the black mass used in Publication III and the residue after leaching without external reductants. Adapted from Publication III, © 2021 The authors, reproduced from Elsevier under CC BY 4.0.

In the experiment without added Cu and Al (Publication III), the Co leaching yield was relatively low (52%). Both Cu and Al scrap additions were found to improve Co leaching yields (Figure 13), and based on the results, Al seemed to have a larger impact per mass unit when compared with Cu. Nevertheless, the most substantial increase in Co yield was obtained by the simultaneous addition of both current collector metals (Figure 13 A).

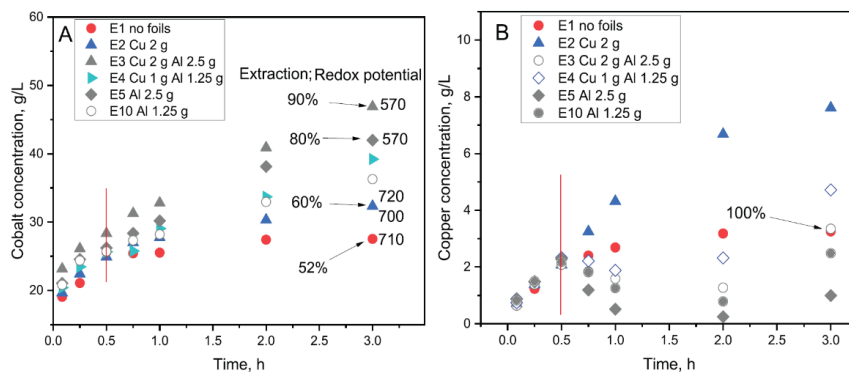


Figure 13. Concentrations of A) Co, B) Cu as a function of time in 2 M H₂SO₄. The time of Cu and Al scrap addition is indicated by vertical red lines. Adapted from Publication III, © 2021 The authors, reproduced from Elsevier under CC BY 4.0.

However, the most important factor related to leaching yield improvements was unlikely to be solely related to the choice of reductant metal, but rather the total added reductive power contained within. The seemingly higher impact of Al can be explained by its higher “electron density”, as Al can donate around 3.5 times the number of electrons per mass unit when compared with Cu (Publication IV; Equation 30).

$$n_{e(Al/Cu)} = \frac{\frac{m}{M_{Al}} \cdot Z_{Al}}{\frac{m}{M_{Cu}} \cdot Z_{Cu}} = \frac{\frac{1}{26.98 \text{ g/mol}} \cdot 3}{\frac{1}{63.55 \text{ g/mol}} \cdot 2} = 3.533 \quad (30)$$

Where $n_{e(Al/Cu)}$ = Relative difference between molar electron amounts donated upon Al and Cu dissolution
 m = mass (g)
 M_x = molar mass of element x (g/mol)
 Z_x = number of electrons donated upon dissolution of one atom of element x

Contrary to the observation stated above, it was found that the current efficiency – the calculated share of donated electrons used in cathode material reduction – of Al was significantly lower than that of Cu (47% for Al vs. 66% for Cu). Such a result was expected as Al is less noble and can consequently participate in side-reactions, *i.e.*, the donated electrons can also be consumed in the reduction reaction of H^+ ions to H_2 gas (Equation 17, Section 2) which is unlikely to further contribute toward cathode material reduction, as discussed in Section 2. In addition to the increased Co leaching yields, Al additions also resulted in a subsequent decrease in the solution Cu concentration (Figure 13 B). This behavior was attributed to Cu cementation on Al particle surfaces, *i.e.*, spontaneous deposition of dissolved Cu^{2+} caused by the reduction potential difference between the two metals (Chernyaev *et al.*, 2022). After initial cementation, Cu was observed to redissolve into the solution, potentially as a response to the depletion of available Al. This hypothesis, however, remains merely speculation, as Al dissolution was not monitored as a part of the study.

Similarly to Publication III, Publication IV also studied the effects of Cu and Al contents of a black mass on cathode material leaching performance, however, with a different approach – using different leaching temperatures (Figure 14) and solution iron concentrations (Figure 15) to facilitate the reductive properties of these metallic fractions already present within the black mass. Within the investigated parameter range (30–70 °C), $T = 70$ °C was found to be the most efficient temperature in terms of cathode metal leaching yields, reaching over 90% yields within two hours (Figure 14 c), whereas experiments at lower temperatures yielded lower transition metal leaching yields (at 50 °C, ~70%; at 30 °C, ~50% for Co, Ni, and Mn). The reason for such low leaching yields was found to be the low solution iron concentration ($[Fe] \sim 200$ mg/L) which impeded efficient electron transfer between reductant metals and the cathode material – as the black mass used in these experiments had a very low iron content (0.1% Fe, Table 3). Increasing the iron concentration from ~200 mg/L (Figure 14) to ~400 mg/L (Figure 15 a and c) improved the cathode metal yields by a notable margin – reaching around 80% yields at $T = 50$ °C – due to the increased concentration of soluble Fe^{2+}/Fe^{3+} ions able to facilitate electron transfer between the reductant metals and cathode material. Nonetheless, a further increase to ~600 mg/L (Figure 15 b and d) did not result in noticeable improvements on

metal yields other than Cu (74% at 50 °C, 400 mg/L Fe, Figure 15 c; 89% at 50 °C, 600 mg/L, Figure 15 d).

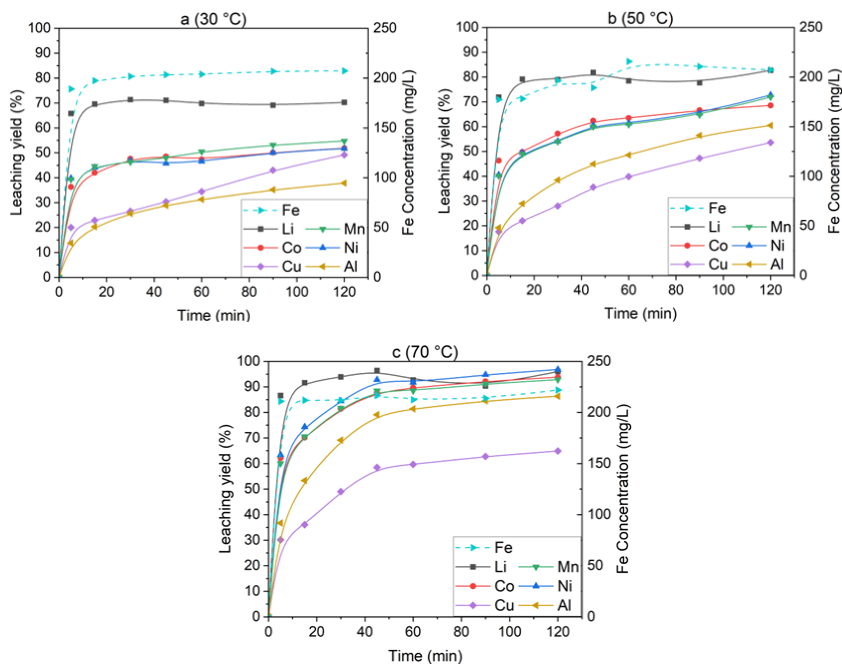


Figure 14. Metal leaching yields at a) 30, b) 50, c) 70 °C in 2 M H₂SO₄. Solid lines indicate metal leaching yields (left Y-axis). Dashed lines illustrate solution iron concentration (right Y-axis). Adapted from Publication IV, © 2024 The authors, reproduced from Elsevier under CC BY 4.0.

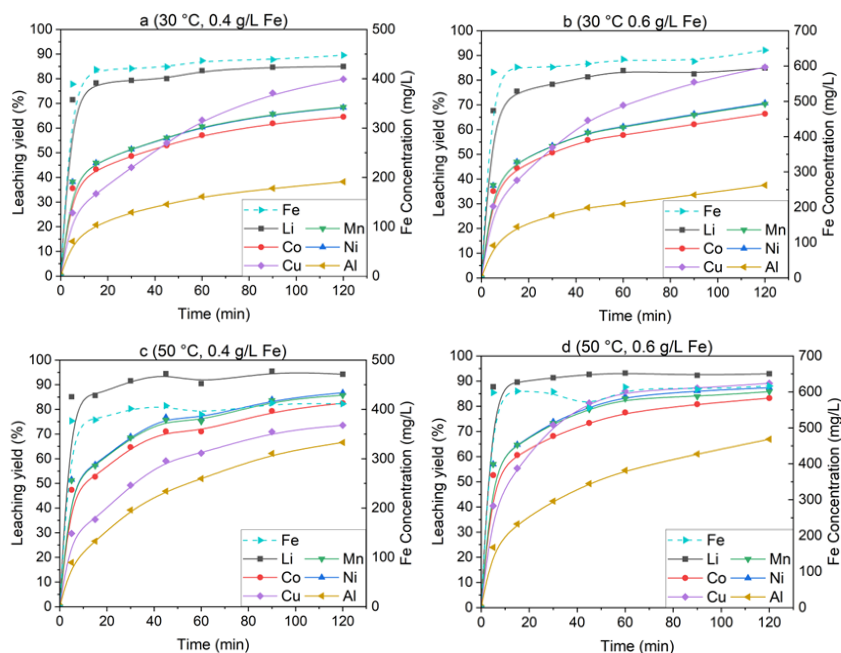


Figure 15. Metal leaching yields with added iron at a) 30 °C, 0.4 g/L total Fe, b) 30 °C, 0.6 g/L total Fe, c) 50 °C, 0.4 g/L total Fe, d) 50 °C, 0.6 g/L total Fe in 2 M H₂SO₄. Solid lines indicate metal leaching yields (left Y-axis). Dashed lines illustrate solution iron concentration (right Y-axis). Adapted from Publication IV, © 2024 The authors, reproduced from Elsevier under CC BY 4.0.

Experiments carried out under these different conditions revealed highly interesting information on the reductant metals behavior. Increasing the temperature did not have a notable effect on Cu dissolution, whereas Al dissolution was strongly accelerated at higher ($T \geq 50$ °C) temperatures. On the other hand, solution iron concentration did not considerably affect Al dissolution, whereas Cu dissolution increased remarkably when iron concentration was increased to 400 mg/L. These findings were interpreted as indicating a difference between the limiting factors of Cu and Al dissolution – Al being limited by surface passivation and reactions related to the oxide layer (Shukla *et al.*, 2023), while Cu is controlled by reactions between metallic Cu and soluble Fe³⁺ ions. Furthermore, none of the experiments in Publications III and IV showed any signs of manganese precipitation – unlike in Publication I. This observation can be explained by the abundance of alternative reductants in the system, as Mn²⁺ oxidation to MnO₂ is thermodynamically less favorable when compared with many of the alternative reactions, *e.g.*, Cu and Al oxidation to Cu²⁺ and Al³⁺ (Equations 7 and 12 in Table 1). The redox potentials measured in Publication III also indicated that the leaching conditions were not oxidizing enough to allow for MnO₂ precipitation ($E \leq 880$ mV vs. SHE).

Notably, Publications III and IV demonstrated that high cathode metal yields can be achieved by carefully considering the raw material contents and modifying the feed compositions accordingly. As discussed above, Publication III added extra Cu and Al into the feed, whereas Publication IV adjusted the solu-

tion iron concentration to facilitate the reductive capabilities of the current collector metals already present within the black mass. The success of both methods with these different raw materials highlights the importance of a thorough knowledge on black mass composition and the ability to adjust the feed accordingly in order to maximize the benefits attainable by current collector utilization – and thereby reduce the demand for external reductants such as H_2O_2 .

4.2.2 Regression modeling

Both Publications III and IV supplemented experimental work with regression modeling. In Publication III, this included deriving an equation to predict Co leaching yields (Equation 31) – as well as for acid consumption and final PLS acidity – based on added Cu and Al masses. For the purposes of this thesis, the Co leaching yield model was further refined to consider molar reductant amounts vs. reducible cathode metal amounts in the feed (Equation 32) for a more convenient comparison with the model created in Publication IV (Equation 33) which predicts Co leaching yields based on a different set of variables – molar amounts of Cu, Fe, and H_2O_2 in the feed, as well as temperature. Both publications considered only linear terms in their models, as quadratic and interaction terms were found to be statistically insignificant. **N.B.**, Equation 33 has been modified from Publication IV to consider iron as a solution concentration in g/L instead of a molar ratio Fe/TM (Transition Metals).

$$Co\ yield\ (\%) = 3.56 \cdot [Cu] + 11.6 \cdot [Al] + 72.5 \quad (31)$$

$$Co\ yield\ (\%) = 269 \cdot [Cu/TM] + 300 \cdot [Al/TM] - 4.97 \quad (32)$$

$$Co\ yield\ (\%) = 0.90 \cdot [T] + 31.4 \cdot [Cu/TM] + 34.2 \cdot [Fe] + 18.5 \cdot [H_2O_2/TM] + 16.6 \quad (33)$$

Where

- [Cu] = Added copper (g)
- [Al] = Added aluminum (g)
- [X/TM] = Molar amount of reductant X in feed divided by the sum of transition metals (Co, Ni, and Mn) molar amounts in feed (mol/mol)
- [T] = Leaching temperature (°C)
- [Fe] = Solution iron concentration (g/L)

Formulating Equation 31 to consider molar reductant additions vs. reducible cathode metals instead of mass units changes the coefficients for Cu and Al by a large margin. Specifically, the coefficients between Cu and Al in the resulting Equation 32 are almost equal (269 for Cu, 300 for Al), whereas the original coefficients reported in Publication III seemed to significantly favor aluminum over copper (3.56 for Cu, 11.6 for Al). Moreover, even the modified equation does not consider the different numbers of electrons donated by the reductant

metals per dissolved atom (2 per Cu, 3 per Al), whereas taking this characteristic into account would likely result in a larger coefficient for Cu due to the smaller number of side-reactions and higher current efficiency associated with Cu dissolution – as discussed above in Section 4.2.1. Furthermore, the coefficient for copper varies largely between the models of Publications III and IV (Equations 32 and 33) – the coefficient of Cu/TM being almost 10 times larger in Equation 32. This could be due to the different temperatures used between the studies (60 °C in Publication III vs. 30–50 °C in Publication IV), as temperature has been shown to have a major effect on reaction kinetics (Levenspiel, 1999, pp 28). It is also possible that since Equation 32 does not consider solution iron concentration, the model assigns the positive effects of iron to Cu and Al – as without these metals, solution iron concentration does not influence cathode metal leaching yields – whereas in Equation 33, the effect of iron is considered separately.

The model created in Publication IV also revealed crucial information regarding the efficiency of copper when compared to hydrogen peroxide. Cu was found to be markedly more efficient as indicated by Figure 16 – likely due to the various side-reactions and decomposition phenomena associated with H_2O_2 , as discussed in Section 2.3.1. This finding emphasizes the benefits of utilizing scrap Cu as a reductant in preference to H_2O_2 .

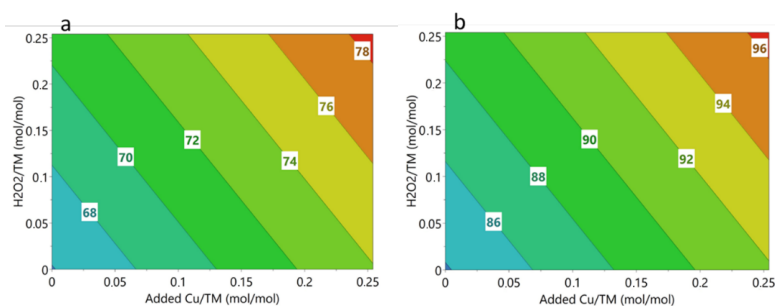


Figure 16. Predicted Co yields (%) with various Cu and H_2O_2 additions at a) $T = 30$ °C, b) $T = 50$ °C, with $[Fe] = 0.4$ g/L. Adopted from Publication IV, © 2024 The authors, reproduced from Elsevier under CC BY 4.0.

4.2.3 Environmental considerations

Sections 4.2.1 and 4.2.2 above have mainly focused on the reductive capabilities of various reductants and their performance in the leaching process. However, the manufacture of chemicals that can be used as reductants inevitably produces CO_2 emissions, and therefore, environmental issues are of high interest as a part of reductant consideration for industrial processes. To illustrate the environmental aspects of selected reductants, Publication III compared the CO_2 emissions associated with the production of H_2O_2 and current collector metals Cu and Al, considering both primary and secondary production (Figure 17). It can be seen that production of H_2O_2 for the reduction and dissolution of one metric tonne of cobalt originating from LCO would result in more than 1 200 kg of CO_2 emissions. Using scrap Cu and Al instead – either contained within black mass

or as a separate feed consisting of production scrap – would avoid these emissions and thereby aid in the carbon footprint reduction of battery recycling processes.

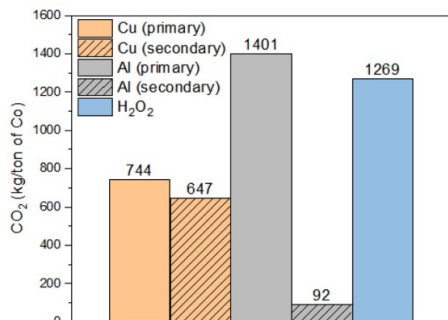


Figure 17. CO₂ amounts emitted in the production of various reductants required for the reduction of 1 tonne of Co (according to Ecoinvent 3.6 database). Adopted from Publication III, © 2021 The authors, reproduced from Elsevier under CC BY 4.0.

The main disadvantage related to the use of Cu and Al as reductants in preference to H₂O₂ is the subsequent need for their removal from the PLS at a later process stage, which will inevitably contribute to the energy consumption and CO₂ emissions of the process. Nonetheless, in the case of copper, there are many efficient and industrially applied state-of-the-art methods to recover the metal from various leach solutions (Schlesinger *et al.*, 2022), whereas excessive amounts of soluble Al could prove problematic due to the shortcomings associated with its removal and recovery, as discussed in Section 2.3.2. The low emissions associated with secondary Al production (Figure 17) also suggest Al separation from black mass and recycling in a dedicated process as a more beneficial alternative than utilizing the metal as a reductant in leaching – a similar approach has also been proposed by Rinne *et al.* (2021). The reductant demand could then be satisfied with the copper contained within the black mass, potentially supported by extra copper scrap additions – originating *e.g.* from battery cell production or other industrial manufacturing facilities – as necessary.

4.2.4 Black mass leaching in the presence of chlorides

Experiments in Publications III and IV were exclusively performed using H₂SO₄ as the lixiviant. Nonetheless, the promising results of Publication II raised the interest to also investigate the use of chloride-containing lixiviants for black mass leaching. One separate leaching experiment for this compendium was conducted using a similar chloride concentration to that found previously efficient for the pure cathode chemicals in Publication II ($T = 50\text{ }^{\circ}\text{C}$, $[\text{H}_2\text{SO}_4] = 3\text{ M}$, $[\text{NaCl}] = 0.2\text{ M}$, S/L = 200 g/L). However, the reactor overflowed soon after black mass introduction as a result of excessive gas generation (Figure 18 a) – due to either H₂ gas produced by a rapid reaction between H⁺ ions and Al (Equation 17, Section 2) or Cl₂ gas evolved as a result of cathode material reduction by Cl⁻ ions (Equations 6 and 18, Section 2). It is likely that both reactions may have contributed to frothing, as considerable amounts of Ni, Mn, Co, and Al were

found to have dissolved within the first 5 minutes (Figure 18 b) – although the calculated yields should only be treated as estimates due to material losses from the overflow. Such a violent reaction raises questions about the compatibility of LIB black mass materials with chloride-containing lixiviants in real-life processes, even at low chloride concentrations (0.2 M NaCl). Nevertheless, the tendency for such intense frothing may also be characteristic for the type of black mass used, as similar incidents have not been reported previously in literature where leaching of LIB waste fractions was studied using 2 M HCl at 80 °C (Takacova *et al.*, 2016) and 4 M HCl at 80 °C (Porvali *et al.*, 2019). Alternatively, S/L ratio may have had a remarkable impact on frothing, as the existing literature used considerably lower S/L ratios – 20 g/L (Takacova *et al.*, 2016) and 50–100 g/L (Porvali *et al.*, 2019) – whereas the experiment in this thesis was conducted with a higher, more industrially attractive S/L ratio (200 g/L).

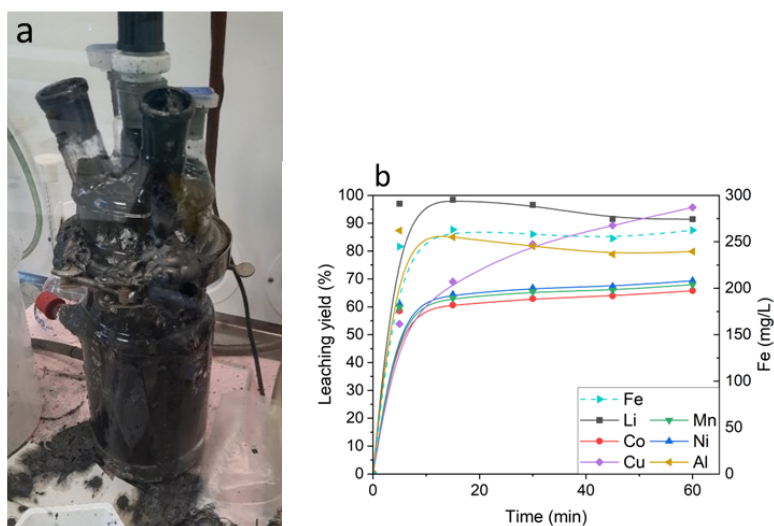


Figure 18. a) Reactor overflow after black mass introduction to the chloride-containing sulfuric acid solution, b) metal leaching yields, $T = 50\text{ }^{\circ}\text{C}$, $[\text{H}_2\text{SO}_4] = 3\text{ M}$, $[\text{NaCl}] = 0.2\text{ M}$. Solid lines indicate metal leaching yields (left Y-axis). Dashed lines illustrate solution iron concentration (right Y-axis).

5. Critical outlook and future prospects

When looking at the results and observations obtained from the research outlined in this thesis, it should be noted that leaching is only one part of a wider hydrometallurgical recycling process. Also, the results obtained using a small-scale laboratory setup are not always directly applicable to a large-scale industrial process. Therefore, it is important to consider the implications of these results and observations in relation to real-life battery recycling processes.

For example, manganese was found to precipitate out of sulfuric acid media when commercial NMC cathode powder was used as the raw material – especially under temperatures of $T \geq 70$ °C (Publication I), implying that this could result in significant Mn losses into the leach residue in the context of a black mass recycling process. Nonetheless, the presence of metallic reductants within black masses was found to inhibit this precipitation (Publication IV), which indicates that such a drawback does not exist in industrial processes, provided that a sufficient supply of thermodynamically more favorable reductants – such as current collector metals Cu and Al – is ensured.

As discussed on several occasions throughout this thesis, metallic reductants have multiple advantages over the traditionally used H_2O_2 , both in terms of reductive efficiency and potentially also regarding environmental impacts. Nonetheless, achieving a complete dissolution simultaneously for both reductants and cathode materials would necessitate a very precise control over the transition metal/reductant metal ratio in the feed – which may not be realistic in industrial operations, especially with varying battery chemistries entering the process. Therefore, as a potentially more beneficial processing strategy, the leach residue could be subjected to a second leaching stage using hydrogen peroxide as an additive. In this kind of process, the dual nature of H_2O_2 as both an oxidant and reductant would be an advantage, as it could dissolve the rest of the metal contents regardless of whether the main metal content in the residue is composed of undissolved cathode material or reductant metals.

Another aspect that should be considered on an industrial scale is cathode material reduction by Cl^- ions and the resulting Cl_2 gas formation. As shown by the results of Publication I, this is a viable interaction with beneficial impacts with respect to cathode metal leaching yields. Nonetheless, the Cl_2 gas generation may pose additional drawbacks in terms of safety and equipment corrosion. Moreover, a high S/L ratio in conjunction with a chloride-containing lixiviant may potentially result in violent frothing with adverse consequences, as demonstrated by the individual black mass leaching experiment conducted in chloride-containing media (Section 4.2.4). Such intense frothing may present challenges

to the development of chloride-based battery recycling processes in the industry, where high S/L ratios are typically preferred. Therefore, further research on the effects of S/L ratio on chloride-based black mass leaching is necessary. Another important aspect for potential future research related to frothing is the impacts of organic battery constituents – especially electrolytes – on frothing behavior. Investigation of black masses with their organic contents removed – *e.g.*, by pyrolysis – focusing on froth formation behavior could be undertaken to determine whether the removal of these compounds prior to leaching would alleviate the associated shortcomings.

Lastly, as always when working with experimental data, all results are subject to potential errors. This is particularly evident when working with industrial black masses due to the inhomogeneity of the raw material, as demonstrated by the relatively large standard deviation values – especially with respect to Cu – outlined in Table 3 (Section 3.2) and previously reported by Porvali *et al.* (2019). Nonetheless, despite the relatively large error margins, all publications included in this thesis show clear trends in relation to the phenomena investigated, and the observations made thereof are believed to be valid and serve as a rigorous foundation for the development of future battery recycling technologies.

6. Conclusions

This thesis investigated the leaching behavior of different kinds of lithium-ion battery raw materials. Publications I and II used pure cathode powders to investigate the leaching mechanisms of LCO and NMC111 cathode materials in sulfate and chloride systems. These principles were then researched in Publications III and IV under more industrially relevant conditions, using industrially produced black mass to study the effects of temperature and various reductants on cathode material leaching performance.

In experiments conducted with pure cathode materials, chloride-containing solutions were found to be marginally more efficient lixiviants when compared with sulfuric acid solutions, as manganese compound precipitation was prevented by provision of an alternative anodic reaction in the form of chlorine gas evolution (Publication I). Nevertheless, as the associated benefits were limited, the risks regarding the Cl_2 gas produced – particularly related to toxicity and equipment corrosion – may outweigh the benefits. This is especially true since manganese compound precipitation was also found to be inhibited in sulfate-based solutions in the presence of metallic reductants commonly found within industrial black masses (Publications III and IV). When compared with leaching experiments using Cl^- ions as the sole reductant (Publication I), experiments using metallic copper as an external reductant exhibited markedly improved leaching kinetics even at relatively mild conditions ($T = 30\text{ }^\circ\text{C}$, $[\text{H}_2\text{SO}_4] = 1\text{ M}$, $[\text{NaCl}] = 0.2\text{ M}$; Publication II), despite the associated CuCl formation. Nonetheless, a subsequent leaching experiment conducted with industrial black mass revealed the potential hazards related to the use of chloride-containing lixiviants, as rapid gas evolution and associated frothing resulted in a reactor overflow. This incident demonstrates that results obtained using pure cathode chemicals cannot be directly assumed to apply to real-life waste fractions, as any impurities contained within such waste can have remarkable effects on the leaching performance.

Leaching experiments performed using sulfate solutions and industrially produced black masses (Publications III and IV) provided new information with respect to current collector metals behavior under various leaching conditions. For example, Al dissolution was found to be enhanced at increased temperatures ($T \geq 50\text{ }^\circ\text{C}$), whereas Cu dissolution rate was much more affected by the solution iron concentration due to the catalyzing effect of the $\text{Fe}^{2+}/\text{Fe}^{3+}$ ion pair – up to 0.4 g/L Fe . Furthermore, statistical analysis of these leaching systems with DoE and regression modeling also provided important information about the reductive capabilities of different reductants, showing a relatively similar

reducing power between Cu and Al (Equation 32) and a much lower reducing power of H_2O_2 when compared with Cu (Equation 33). Furthermore, a brief consideration of carbon dioxide emissions associated with Cu, Al, and H_2O_2 production indicated current collector metals to be a potentially more environmental alternative over H_2O_2 , especially considering the amount of extra H_2O_2 required to achieve the same degree of cathode material dissolution – as demonstrated by Equation 33.

References

- Alemrajabi, M., Karlsson, I., Sjö Dahl, R., Nehrenheim, E., Petranikova, M., Tunsu, C., 2022. Process for the recovery of cathode materials in the recycling of batteries by removing aluminum and iron, US11509000B2.
- Amalia, D., Singh, P., Zhang, W., Nikoloski, A.N., 2023. Discharging of spent cylindrical lithium-ion batteries in sodium hydroxide and sodium chloride for a safe recycling process. *JOM* 75, 4946–4957. <https://doi.org/10.1007/s11837-023-06093-x>.
- Baade, W.F., Parekh, U.N., Raman, V.S., 2001. Hydrogen. In *Kirk-Othmer Encyclopedia of Chemical Technology*. <https://doi.org/10.1002/0471238961.0825041803262116.a01.pub2>.
- Billy, E., Joulié, M., Laucournet, R., Boulineau, A., De Vito, E., Meyer, D., 2018. Dissolution mechanisms of $\text{LiNi}_{1/3}\text{Mn}_{1/3}\text{Co}_{1/3}\text{O}_2$ positive electrode material from lithium-ion batteries in acid solution. *ACS Appl. Mater. Interfaces* 10, 16424–16435. <https://doi.org/10.1021/acsami.8b01352>.
- Bishoyi, S.S., Behera, S.K., 2024. Fabrication and electrochemical performance of Si-C composite nanostructures with SiO_2 sacrificial agent for LIB anode. *J. Alloys Compd.* 982, 173766. <https://doi.org/10.1016/j.jallcom.2024.173766>.
- Bree, G., Horstman, D., Low, C.T.J., 2023. Light-weighting of battery casing for lithium-ion device energy density improvement. *J. Energy Storage* 68, 107852. <https://doi.org/10.1016/j.est.2023.107852>.
- Carreira, A.R.F., Nogueira, A.F.M., Rocha, I.L.D., Sosa, F., da Costa Lopes, A.M., Passos, H., Schaeffer, N., Coutinho, J.A.P., 2024. Repurposing kraft black liquor as reductant for enhanced lithium-ion battery leaching. *ChemSusChem* 17, e202301801. <https://doi.org/10.1002/cssc.202301801>.
- Castro, F. D., Vaccari, M., Cutaia, L., 2022. Valorization of resources from end-of-life lithium-ion batteries: A review. *Crit. Rev. Env. Sci. Technol.* 52, 2060–2103. <https://doi.org/10.1080/10643389.2021.1874854>.
- Cattaneo, P., Callegari, D., Merli, D., Tealdi, C., Vadivel, D., Milanese, C., Kapelyushko, V., D'Aprile, F., Quartarone, E., 2023. Sorting, characterization, environmentally friendly recycling, and reuse of components from end-of-life 18650 Li ion batteries. *Adv. Sustainable Syst.* 7, 2300161. <https://doi.org/10.1002/adsu.202300161>.
- Cerrillo-Gonzalez, M.M., Villen-Guzman, M., Vereda-Alonso, C., Gomez-Lahoz, C., Rodriguez-Maroto, J.M., Paz-Garcia, J.M., 2020. Recovery of Li and Co from

- LiCoO₂ via hydrometallurgical–electrodialytic treatment. *Appl. Sci.* 10, 2367. <https://doi.org/10.3390/app10072367>.
- Che, H., Wang, J., Gao, X., Chen, J., Wang, P., Liu, B., Ao, Y., 2022. Regulating directional transfer of electrons on polymeric g-C₃N₅ for highly efficient photocatalytic H₂O₂ production. *J. Colloid Interface Sci.* 627, 739–748. <https://doi.org/10.1016/j.jcis.2022.07.080>.
- Chen, M., Wang, R., Qi, Y., Han, Y., Wang, R., Fu, J., Meng, F., Huang, J., Shu, J., 2021. Cobalt and lithium leaching from waste lithium ion batteries by glycine. *J. Power Sources* 482, 228942. <https://doi.org/10.1016/j.jpowsour.2020.228942>.
- Chen, X., Guo, C., Ma, H., Li, J., Zhou, T., Cao, L., Kang, D., 2018. Organic reductants based leaching: A sustainable process for the recovery of valuable metals from spent lithium ion batteries. *Waste Manage.* 75, 459–468. <https://doi.org/10.1016/j.wasman.2018.01.021>.
- Chen, Y., Chang, D., Liu, N., Hu, F., Peng, C., Zhou, X., He, J., Jie, Y., Wang, H., Wilson, B.P., Lundström, M., 2019. Biomass-assisted reductive leaching in H₂SO₄ medium for the recovery of valuable metals from spent mixed-type lithium-ion batteries. *JOM* 71, 4465–4472. <https://doi.org/10.1007/s11837-019-03775-3>.
- Chernyaev, A., Wilson, B.P., Lundström, M., 2021. Study on valuable metal incorporation in the Fe–Al precipitate during neutralization of LIB leach solution. *Sci. Rep.* 11, 23283. <https://doi.org/10.1038/s41598-021-02019-2>.
- Chernyaev, A., Zou, Y., Wilson, B.P., Lundström, M., 2022. The interference of copper, iron and aluminum with hydrogen peroxide and its effects on reductive leaching of LiNi_{1/3}Mn_{1/3}Co_{1/3}O₂. *Sep. Purif. Technol.* 281, 119903. <https://doi.org/10.1016/j.seppur.2021.119903>.
- Chernyaev, A., Zhang, J., Seisko, S., Louhi-Kultanen, M., Lundström, M., 2023. Fe³⁺ and Al³⁺ removal by phosphate and hydroxide precipitation from synthetic NMC Li-ion battery leach solution. *Sci. Rep.* 13, 21445. <https://doi.org/10.1038/s41598-023-48247-6>.
- Chernyaev, A., Kobets, A., Liivand, K., Tesfaye, F., Hannula, P., Kallio, T., Hupa, L., Lundström, M., 2024. Graphite recovery from waste Li-ion battery black mass for direct re-use. *Miner. Eng.* 208, 108587. <https://doi.org/10.1016/j.mineng.2024.108587>.
- Cornelio, A., Zanoletti, A., Bontempi, E., 2024. Recent progress in pyrometallurgy for the recovery of spent lithium-ion batteries: A review of state-of-the-art developments. *Curr. Opin. Green Sustainable Chem.* 46, 100881. <https://doi.org/10.1016/j.cogsc.2024.100881>.
- Drüe, M., Seyring, M., Kozlov, A., Song, X., Schmid-Fetzer, R., Rettenmayr, M., 2013. Thermodynamic stability of Li₂C₂ and LiC₆. *J. Alloys Compd.* 575, 403–407. <https://doi.org/10.1016/j.jallcom.2013.06.001>.

- Dutrizac, J.E., Monhemius, A.J., 1986. Iron Control in Hydrometallurgy, Ellis Horwood Limited, Chichester. ISBN: 0-7458-0010-6.
- Ehrlich, G.M., 2002. Lithium-ion batteries. In Handbook of Batteries 3rd ed., McGraw-Hill, New York, USA, pp 35.1, ISBN: 0-07-135978-8.
- Ellen MacArthur Foundation, 2021. The butterfly diagram: visualising the circular economy. <https://www.ellenmacarthurfoundation.org/circular-economy-diagram>. Accessed 7.1.2025.
- Eul, W., Moeller, A., Steiner, N., 2001. Hydrogen peroxide. In Kirk-Othmer Encyclopedia of Chemical Technology. <https://doi.org/10.1002/0471238961.0825041808051919.a01.pub2>.
- European Commission, 2020. Batteries Europe ETIP WG2: raw materials and recycling roadmap. https://energy.ec.europa.eu/system/files/2021-02/raw_materials_and_recycling_roadmap_3.pdf.
- European Commission, 2023a. Study on the critical raw materials for the EU 2023 – Final report. <https://data.europa.eu/doi/10.2873/725585>. Accessed 11.11.2024.
- European Commission, 2023b. Regulation (EU) 2023/1542 of the European Parliament and of the Council of 12 July 2023 concerning batteries and waste batteries, amending Directive 2008/98/EC and Regulation (EU) 2019/1020 and repealing Directive 2006/66/EC. <http://data.europa.eu/eli/reg/2023/1542/2024-07-18>. Accessed 11.11.2024.
- European Commission, 2024. Directive 2008/98/EC of the european parliament and of the council of 19 November 2008 on waste and repealing certain directives. <https://eur-lex.europa.eu/legal-content/EN/TXT/?uri=CELEX%3A02008L0098-20240218>. Accessed 02.01.2025.
- Ferreira, D.A., Prados, L.M.Z., Majuste, D., Mansur, M.B., 2009. Hydrometallurgical separation of aluminium, cobalt, copper and lithium from spent Li-ion batteries. J. Power Sources 187, 238–246. <https://doi.org/10.1016/j.jpowsour.2008.10.077>.
- Fritz, J.J., 1982. Solubility of cuprous chloride in various soluble aqueous chlorides. J. Chem. Eng. Data 27, 188–193. <https://doi.org/10.1021/je00028a027>.
- Gao, W., Zhang, X., Zheng, X., Lin, X., Cao, H., Zhang, Yi., Sun, Z., 2017. Environ. Sci. Technol. 51, 1662–1669. <https://doi.org/10.1021/acs.est.6b03320>.
- Ghassa, S., Farzanegan, A., Gharabaghi, M., Abdollahi, H., 2020. The reductive leaching of waste lithium ion batteries in presence of iron ions: Process optimization and kinetics modelling. J. Cleaner Prod. 262, 121312. <https://doi.org/10.1016/j.jclepro.2020.121312>.
- Gil-Lozano, C., Davila, A.F., Losa-Adams, E., Fairén, A.G., Gago-Duport, L., 2017. Quantifying Fenton reaction pathways driven by self-generated H₂O₂ on pyrite surfaces. Sci. Rep. 7, 43703. <https://doi.org/10.1038/srep43703>.

- Gilmour, S.G., 2010. Response surface design. In Encyclopedia of Research Design. <https://doi.org/10.4135/9781412961288.n387>.
- Gopalakrishnan, R., Goutam, S., Oliveira, L.M., Timmermans, J., Omar, N., Messagie, M., Van den Bossche, P., van Mierlo, J., 2016. A comprehensive study on re-chargeable energy storage technologies. *J. Electrochem. Energy Convers. Storage* 13, 040801. <https://doi.org/10.1115/1.4036000>.
- Greenwood, N.N., Earnshaw, A., 1997. Chemistry of the elements 2nd edition, Butterworth-Heinemann, Oxford, pp 792–793, ISBN: 978-0-0805-0109-3.
- Hao, O.J., Davis, A.P., Chang, P.H., 1991. Kinetics of manganese(ii) oxidation with chlorine. *J. Environ. Eng.* 117, 359–374. [https://doi.org/10.1061/\(ASCE\)0733-9372\(1991\)117:3\(359\)](https://doi.org/10.1061/(ASCE)0733-9372(1991)117:3(359)).
- Harper, G., Sommerville, R., Kendrick, E., Driscoll, L., Slater, P., Stolkin, R., Walton, A., Christensen, P., Heidrich, O., Lambert, S., Abbott, A., Ryder, K., Gaines, L., Anderson, P., 2019. Recycling lithium-ion batteries from electric vehicles. *Nature* 575, 75–86. <https://doi.org/10.1038/s41586-019-1682-5>.
- Harris, B., White, C., 2021. Process for the recovery of cobalt, lithium, and other metals from spent lithium-based batteries and other feeds, US2021/0079495A1.
- Hashemzadeh, M., Dixon, D.G., Liu, W., 2019. Modelling the kinetics of chalcocite leaching in acidified cupric chloride media under fully controlled pH and potential. *Hydrometallurgy* 189, 105114. <https://doi.org/10.1016/j.hydromet.2019.105114>.
- Hayagan, N., Gaalich, I., Loubet, P., Croguennec, L., Aymonier, C., Philippot, G., Olchowka, J., 2024. Batteries Supercaps e202400120. <https://doi.org/10.1002/batt.202400120>.
- He, B., Zheng, H., Tang, K., Xi, P., Li, M., Wei, L., Guan, Q., 2024. A comprehensive review of lithium-ion battery (LiB) recycling technologies and industrial market trend insights. *Recycling* 9, 9. <https://doi.org/10.3390/recycling9010009>.
- Herreros, O., Quiroz, R., Restovic, A., Viñals, J., 2005. Dissolution kinetics of metallic copper with CuSO₄–NaCl–HCl. *Hydrometallurgy* 77, 183–190. <https://doi.org/10.1016/j.hydromet.2004.11.010>.
- Hossain, M.H., Chowdhury, M.A., Hossain, N., Islam, M.A., Mobarak, M.H., 2023. Advances of lithium-ion batteries anode materials—a review. *Chem. Eng. J. Adv.* 16, 100569. <https://doi.org/10.1016/j.cej.2023.100569>.
- IEA, 2024. Global EV Outlook 2024, IEA, Paris. <https://www.iea.org/reports/global-ev-outlook-2024>.
- Jantunen, N., Virolainen, S., Sainio, T., 2022. Direct production of Ni–Co–Mn mixtures for cathode precursors from cobalt-rich lithium-ion battery leachates by solvent extraction. *Metals* 12, 1445. <https://doi.org/10.3390/met12091445>.

- Jena, K.K., AlFantazi, A., Mayyas, A.T., 2021. Comprehensive review on concept and recycling evolution of lithium-ion batteries (LIBs). *Energy Fuels* 35, 18257–18284. <https://doi.org/10.1021/acs.energyfuels.1c02489>.
- Ji, H., Wang, J., Ma, J., Cheng, H., Zhou, G., 2023. Fundamentals, status and challenges of direct recycling technologies for lithium ion batteries. *Chem. Soc. Rev.* 52, 8194. <https://doi.org/10.1039/D3CS00254C>.
- Joulié, M., Billy, E., Laucournet, R., Meyer, D., 2017. Current collectors as reducing agent to dissolve active materials of positive electrodes from Li-ion battery wastes. *Hydrometallurgy* 169, 426–432. <https://doi.org/10.1016/j.hydromet.2017.02.010>.
- Kang, H., Jung, S., Kim, H., An, J., Hong, J., Yeom, S., Hong, T., 2025. Life-cycle environmental impacts of reused batteries of electric vehicles in buildings considering battery uncertainty. *Renewable Sustainable Energy Rev.* 207, 114936. <https://doi.org/10.1016/j.rser.2024.114936>.
- Kim, E., Ahn, T., Kim, T., 2022. New method for selective recovery of manganese from NCM-based cathode material of spent Li-ion batteries. *Geosyst. Eng.* 25, 143–149. <https://doi.org/10.1080/12269328.2022.2119610>.
- Kivelä, P., Ekman, P., Lappalainen, E., Haapala, K., Kauppinen, P., Ekman, K., 2023. Method for processing black mass to battery chemicals, EP4245869A1.
- Kong, L., Wang, Z., Shi, Z., Hu, X., Liu, A., Tao, W., Wang, B., Wang, Q., 2023. Leaching valuable metals from spent lithium-ion batteries using the reducing agent methanol. *Environ. Sci. Pollut. Res.* 30, 4258–4268. <https://doi.org/10.1007/s11356-022-22414-0>.
- Latini, D., Vaccari, M., Lagnoni, M., Orefice, M., Mathieux, F., Huisman, J., Tognotti, L., Bertei, A., 2022. A comprehensive review and classification of unit operations with assessment of outputs quality in lithium-ion battery recycling. *J. Power Sources* 546, 231979. <https://doi.org/10.1016/j.jpowsour.2022.231979>.
- Larouche, F., Tedjar, F., Amouzegar, K., Houlachi, G., Bouchard, P., Demopoulos, G.P., Zaghbi, K., 2020. Progress and status of hydrometallurgical and direct recycling of li-ion batteries and beyond. *Materials* 13, 801. <https://doi.org/10.3390/ma13030801>.
- Levenspiel, O., 1999. *Chemical reaction engineering* 3rd edition, John Wiley & Sons, USA. ISBN 978-0-471-25424-9.
- Li, G., Hao, H., Zhuang, Y., Wang, Z., Shi, B., 2019. Powdered activated carbon enhanced manganese(II) removal by chlorine oxidation. *Water Res.* 156, 287–296. <https://doi.org/10.1016/j.watres.2019.03.027>.

- Li, P., Luo, S., Zhang, L., Liu, Q., Wang, Y., Lin, Y., Xu, C., Guo, J., Cheali, P., Xia, X., 2024. Progress, challenges, and prospects of spent lithium-ion batteries recycling: A review. *J. Energy Chem.* 89, 144–171. <https://doi.org/10.1016/j.jechem.2023.10.012>.
- Livvand, K., Sainio, J., Wilson, B.P., Kruusenberg, I., Lundström, M., 2023. Overlooked residue of Li-ion battery recycling waste as high-value bifunctional oxygen electrocatalyst for Zn-air batteries. *Appl. Catal., B* 332, 122767. <https://doi.org/10.1016/j.apcatb.2023.122767>.
- Liu, C., Lin, J., Cao, H., Zhang, Y., Sun, Z., 2019. Recycling of spent lithium-ion batteries in view of lithium recovery: A critical review. *J. Cleaner Prod.* 228, 801–813. <https://doi.org/10.1016/j.jclepro.2019.04.304>.
- Liu, F., Peng, C., Porvali, A., Wang, Z., Wilson, B.P., Lundström, M., 2019. Synergistic recovery of valuable metals from spent nickel–metal hydride batteries and Lithium-ion batteries. *ACS Sustain. Chem. Eng.* 7, 16103–16111. <https://doi.org/10.1021/acssuschemeng.9b02863>.
- Liu, Y., Zhao, C., Du, J., Zhang, X., Chen, A., Zhang, Q., 2023. Research Progresses of Liquid Electrolytes in Lithium-Ion Batteries. *Small* 19, 2205315. <https://doi.org/10.1002/sml.202205315>.
- Lu, J., Tian, X., Zhou, Y., Zhu, Y., Tang, Z., Ma, B., Wu, G., Jiang, T, Tu, X., Chen, G.Z., 2019. A novel “holey-LFP / graphene / holey-LFP” sandwich nanostructure with significantly improved rate capability for lithium storage. *Electrochim. Acta* 320, 134566. <https://doi.org/10.1016/j.electacta.2019.134566>.
- Lundström, M., Aromaa, J., Forsén, O., Hyvärinen, O., Barker, M.H., 2005. Leaching of chalcopyrite in cupric chloride solution. *Hydrometallurgy* 77, 89–95. <https://doi.org/10.1016/j.hydromet.2004.10.013>.
- Lundström, M., Liipo, J., Taskinen, P., Aromaa, J., 2016. Copper precipitation during leaching of various copper sulfide concentrates with cupric chloride in acidic solutions. *Hydrometallurgy* 166, 136–142. <https://doi.org/10.1016/j.hydromet.2016.10.017>.
- Lv, W., Wang, Z., Cao, H., Zheng, X., Jin, W., Zhang, Y., Sun, Zhi., 2018. A sustainable process for metal recycling from spent lithium-ion batteries using ammonium chloride. *Waste Manage.* 79, 545–553. <https://doi.org/10.1016/j.wasman.2018.08.027>.
- Ma, H., Wang, X., Fu, Y., Zhang, Y., Ma, C., Dong, X., Yu, Z., 2019. Study on the fabrication and photoelectrochemical performance of the F– doped Ti/Co₃O₄ electrodes with n-type semiconductor characteristics. *J Solid State Electrochem* 23, 1767–1777. <https://doi.org/10.1007/s10008-019-04256-y>.
- Makuza, B., Tian, Q., Guo, X., Chattopadhyay, K., Yu, D., 2021. Pyrometallurgical options for recycling spent lithium-ion batteries: A comprehensive review. *J. Power Sources* 491, 229622. <https://doi.org/10.1016/j.jpowsour.2021.229622>.

- Manoharan, S., Mahalakshmi, B., Govindaraj, V., Vidyalakshmi, R., 2024. The evolution of mobile phone batteries: from Ni-Cd to Li-ion. International Conference on Science Technology Engineering and Management (ICSTEM), Coimbatore, India, pp. 1-6. <https://doi.org/10.1109/ICSTEM61137.2024.10560523>.
- Mao, J., Ye, C., Zhang, S., Xie, F., Zeng, R., Davey, K., Guo, Z., Qiao, S., 2022. Toward practical lithium-ion battery recycling: adding value, tackling circularity and recycling-oriented design. *Energy Environ. Sci.* 15, 2732–2752. <https://doi.org/10.1039/D2EE00162D>.
- Matsumoto, F., Gunji, T., 2022. Water in lithium-ion batteries, Springer Singapore, pp 1, <https://doi.org/10.1007/978-981-16-8786-0>.
- Meshram, P., Pandey, B.D., Mankhand, T.R., 2015. Hydrometallurgical processing of spent lithium ion batteries (LIBs) in the presence of a reducing agent with emphasis on kinetics of leaching. *Chem. Eng. J.* 281, 418–427. <https://doi.org/10.1016/j.cej.2015.06.071>.
- Mossali, E., Picone, N., Gentilini, L., Rodriquez, O., Pérez, J.M., Colledani, M., 2020. Lithium-ion batteries towards circular economy: A literature review of opportunities and issues of recycling treatments. *J. Environ. Manage.* 264, 110500. <https://doi.org/10.1016/j.jenvman.2020.110500>.
- MSE Supplies, 2024. MSE PRO Lithium Nickel Manganese Cobalt Oxide NMC 111 Cathode Powder 500g, $\text{Li}_{1.05}\text{Ni}_{0.33}\text{Mn}_{0.33}\text{Co}_{0.33}\text{O}_2$. <https://www.msесupplies.com/products/mse-pro-lithium-nickel-manganese-cobalt-oxide-nmc-111-cathode-powder-500g>. Accessed 30.10.2024.
- Müller, H., 2000. Sulfuric acid and sulfur trioxide. In *Ullmann's Encyclopedia of Industrial Chemistry*. https://doi.org/10.1002/14356007.a25_635.
- Nan, J., Han, D., Zuo, X., 2005. Recovery of metal values from spent lithium-ion batteries with chemical deposition and solvent extraction. *J. Power Sources* 152, 278–284. <https://doi.org/10.1016/j.jpowsour.2005.03.134>.
- Nobel Prize Outreach, 2024. The Nobel Prize in Chemistry 2019. www.nobelprize.org/prizes/chemistry/2019/summary. Accessed 30.10.2024.
- Or, T., Gourley, S.W.D., Kaliyappan, K., Yu, A., Chen, Z., 2020. Recycling of mixed cathode lithium-ion batteries for electric vehicles: Current status and future outlook. *Carbon Energy* 2, 6–43. <https://doi.org/10.1002/cey2.29>.
- Peng, C., Hamuyuni, J., Wilson, B.P., Lundström, M., 2018. Selective reductive leaching of cobalt and lithium from industrially crushed waste Li-ion batteries in sulfuric acid system. *Waste Manage.* 76, 582–590. <https://doi.org/10.1016/j.wasman.2018.02.052>.
- Peng, C., Liu, F., Aji, A.T., Wilson, B.P., Lundström, M., 2019. Extraction of Li and Co from industrially produced Li-ion battery waste – Using the reductive power of waste itself. *JOM* 72, 790–799. <https://doi.org/10.1016/j.wasman.2019.06.048>.

- Pisarczyk, K., 2005. Manganese Compounds. In Kirk-Othmer Encyclopedia of Chemical Technology.
<https://doi.org/10.1002/0471238961.1301140716091901.a01.pub2>.
- Porvali, A., Aaltonen, M., Ojanen, S., Velazquez-Martinez, O., Eronen, E., Liu, F., Wilson, B.P., Serna-Guerrero, R., Lundström, M., 2019. Mechanical and hydrometallurgical processes in HCl media for the recycling of valuable metals from Li-ion battery waste. *Resour. Conserv. Recycl.* 142, 257–266.
<https://doi.org/10.1016/j.resconrec.2018.11.023>.
- Porvali, A., Chernyaev, A., Shukla, S., Lundström, M., 2020a. Lithium ion battery active material dissolution kinetics in Fe(II)/Fe(III) catalyzed Cu-H₂SO₄ leaching system. *Sep. Purif. Technol.* 236, 116305. <https://doi.org/10.1016/j.seppur.2019.116305>.
- Porvali, A., Shukla, S., Lundström, M., 2020b. Low-acid leaching of lithium-ion battery active materials in Fe-catalyzed Cu-H₂SO₄ system. *Hydrometallurgy* 195, 105408. <https://doi.org/10.1016/j.hydromet.2020.105408>.
- Pudas, J., Erkkilä, A., Viljamaa, J., 2015. Battery Recycling Method, US8979006B2.
- Puvvada, G.V.K., Sridhar, R., Lakshmanan, V.I., 2003. Chloride metallurgy: PGM recovery and titanium dioxide production. *JOM* 55, 38–41.
<https://doi.org/10.1007/s11837-003-0103-1>.
- Raudsepp, R., Beattie, M.J.V., 1986. Iron control in chloride systems. In *Iron Control in Hydrometallurgy*, Eds. J.E. Dutrizac and A.J. Monhemius, Ellis Horwood Limited, Chichester, pp 169. ISBN: 0-7458-0010-6.
- Rinne, M., Elomaa, H., Porvali, A., Lundström, M., 2021. Simulation-based life cycle assessment for hydrometallurgical recycling of mixed LIB and NiMH waste. *Resour. Conserv. Recycl.* 170, 105586. <https://doi.org/10.1016/j.resconrec.2021.105586>.
- Rinne, T., Saeed, M., Serna-Guerrero, R., 2024. Quantifying the degree of selectivity in a Flocculation-Flotation process of LiCoO₂ and graphite using scanning electron microscopy and image processing analysis. *Miner. Eng.* 209, 108644.
<https://doi.org/10.1016/j.mineng.2024.108644>.
- Roy, J.J., Phuong, D.M., Verma, V., Chaudhary, R., Carboni, M., Meyer, D., Cao, B., Srinivasan, M., 2024. Direct recycling of Li-ion batteries from cell to pack level: Challenges and prospects on technology, scalability, sustainability, and economics. *Carbon energy* e492, <https://doi.org/10.1002/cey2.492>.
- Scheunis, L., Callebaut, W., 2024. Process for the recovery of lithium, US11952643B2.
- Schmittinger, P., Florkiewicz, T., Curlin, L.C., Lüke, B., Scannell, R., Navin, T., Zelfel, E. and Bartsch, R., 2011. Chlorine. In *Ullmann's Encyclopedia of Industrial Chemistry*. https://doi.org/10.1002/14356007.a06_399.pub3.

- Schlesinger, M.E., Sole, K.C., Davenport, W.G., Alvear Flores, G.R.F., 2022. Extractive metallurgy of copper 6th edition, Elsevier, ISBN 9780128218754.
- Seisko, S., Aromaa, J., Lundström, M., 2019. Features affecting the cupric chloride leaching of gold. *Miner. Eng.* 137, 94–101.
<https://doi.org/10.1016/j.mineng.2019.03.030>.
- Shi, M., Ren, Y., Cao, J., Kuang, Z., Zhuo, X., Xie, H., 2023. Current situation and development prospects of discharge pretreatment during recycling of lithium-ion batteries: a review. *Batteries Supercaps* 7, e202300477.
<https://doi.org/10.1002/batt.202300477>.
- Shin, S.M., Kim, N.H., Sohn, J.S., Yang, D.H., Kim, Y.H., 2005. Development of a metal recovery process from Li-ion battery wastes. *Hydrometallurgy* 79, 172–181. <https://doi.org/10.1016/j.hydromet.2005.06.004>.
- Shina, S., 2022. Data Presentations, Statistical Distributions, Quality Tools, and Relationship to DoE. In: *Industrial Design of Experiments*. Springer, Cham.
https://doi.org/10.1007/978-3-030-86267-1_1.
- Shinova, E., Stoyanova, R., Zhecheva, E., Ortiz, G.F., Lavela, P., Tirado, J.L., 2008. Cationic distribution and electrochemical performance of $\text{LiCo}_{1/3}\text{Ni}_{1/3}\text{Mn}_{1/3}\text{O}_2$ electrodes for lithium-ion batteries. *Solid State Ionics* 179, 2198–2208.
<https://doi.org/10.1016/j.ssi.2008.07.026>.
- Shukla, S., Chernyaev, A., Halli, P., Aromaa, J., Lundström, M., 2023. Leaching of waste pharmaceutical blister package aluminium in sulphuric acid media. *Metals* 13, 1118. <https://doi.org/10.3390/met13061118>.
- Sohn, J-S., Shin, S-M., Yang, D-H., Kim, S-K., Lee, C-K., 2006. Comparison of two acidic leaching processes for selecting the effective recycle process of spent lithium ion battery. *Geosyst. Eng.* 9, 1–6.
<https://doi.org/10.1080/12269328.2006.10541246>.
- Sristava, A., Meshram, A., 2023. On trending technologies of aluminium dross recycling: A review. *Process Saf. Environ. Prot.* 171, 38–54.
<https://doi.org/10.1016/j.psep.2023.01.010>.
- Staudacher, M., Lyon, T., Peuker, U., 2024. challenges in the recycling of battery casing materials. *Chem. Ing. Tech.* 96, 932–940.
<https://doi.org/10.1002/cite.202300134>.
- Takacova, Z., Havlik, T., Kukurugya, F., Orac, D., 2016. Cobalt and lithium recovery from active mass of spent Li-ion batteries: Theoretical and experimental approach. *Hydrometallurgy* 163, 9–17. <http://dx.doi.org/10.1016/j.hydromet.2016.03.007>.
- Torkaman, R., Asadollahzadeh, M., Torab-Mostaedi, M., Maragheh, M.G., 2017. Recovery of cobalt from spent lithium ion batteries by using acidic and basic extractants in solvent extraction process. *Sep. Purif. Technol.* 186, 318–325.
<https://doi.org/10.1016/j.seppur.2017.06.023>.

- Trivedi, S., Pamidi, V., Bautista, S.P., Shamsudin, F.N.A., Weil, M., Barpanda, P., Bresser, D., Fichtner, M., 2024. Water-soluble inorganic binders for lithium-ion and sodium-ion batteries. *Adv. Energy Mater.* 14, 2303338. <https://doi.org/10.1002/aenm.202303338>.
- Tu, S., 1993. Effects of KCl on solubility and bioavailability of Mn in soil and some reactions of birnessite in the presence of some Mn compounds. Doctoral thesis, University of Manitoba, Department of Soil Science, Winnipeg, 112 p.
- Umicore, 2023. Umicore battery recycling: Capturing profitable growth and enabling a circular and low-carbon battery value chain. <https://www.umi-core.com/en/newsroom/news/umicore-battery-recycling>. Accessed 30.10.2024
- Velázquez-Martínez, O., Valio, J., Santasalo-Aarnio, A., Reuter, M., Serna-Guerrero, R., 2019. A critical review of lithium-ion battery recycling processes from a circular economy perspective. *Batteries* 5, 68. <https://doi.org/10.3390/batteries5040068>.
- Volta, A., 1800. On the electricity excited by the mere contact of conducting substances of different kinds. *Abstracts of the Papers Printed in the Philosophical Transactions of the Royal Society of London* 1, 27–29. <http://www.jstor.org/stable/109515>. Accessed 30.10.2024.
- Wang, H., Fridrich, B., 2015. Development of a highly efficient hydrometallurgical recycling process for automotive li-ion batteries. *J. Sustain. Metall.* 1, 168–178. <https://doi.org/10.1007/s40831-015-0016-6>.
- Wang, S., Zhang, Z., Lu, Z., Xu, Z., 2020. A novel method for screening deep eutectic solvent to recycle the cathode of Li-ion batteries. *Green Chem.* 22, 4473–4482. <https://doi.org/10.1039/D0GC00701C>.
- Warner, J.T., 2015. *The handbook of lithium-ion battery pack design: chemistry, components, types and terminology*, Elsevier, Amsterdam, pp 76, ISBN: 978-0-12-801456-1.
- Wesselborg, T., Virolainen, S., Sainio, T., 2021. Recovery of lithium from leach solutions of battery waste using direct solvent extraction with TBP and FeCl₃. *Hydrometallurgy* 202, 105593. <https://doi.org/10.1016/j.hydromet.2021.105593>.
- Wilke, C., Werner, D.M., Kaas, A., Peuker, U.A., 2023. Influence of the Crusher Settings and a Thermal Pre-Treatment on the Properties of the Fine Fraction (Black Mass) from Mechanical Lithium-Ion Battery Recycling. *Batteries* 9, 514. <https://doi.org/10.3390/batteries9100514>.
- Wold, S., Sjöström, M., Eriksson, L., 2001. PLS-regression: a basic tool of chemometrics. *Chemom. Intell. Lab. Syst.* 58, 109–130. [https://doi.org/10.1016/S0169-7439\(01\)00155-1](https://doi.org/10.1016/S0169-7439(01)00155-1).

- Xu, P., Tan, D.H.S., Jiao, B., Gao, H., Yu, X., Chen, Z., 2023. A materials perspective on direct recycling of lithium-ion batteries: principles, challenges and opportunities. *Adv. Funct. Mater.* 33, 2213168. <https://doi.org/10.1002/adfm.202213168>.
- Xuan, W., Otsuki, A., Chagnes, A., 2019. Investigation of the leaching mechanism of NMC 811 (LiNi_{0.8}Mn_{0.1}Co_{0.1}O₂) by hydrochloric acid for recycling lithium ion battery cathodes. *RSC adv.* 9, 38612. <https://doi.org/10.1039/c9ra06686a>.
- Xuan, W., de Souza Braga, A., Korbel, C., Chagnes, A., 2021. New insights in the leaching kinetics of cathodic materials in acidic chloride media for lithium-ion battery recycling. *Hydrometallurgy* 204, 105705. <https://doi.org/10.1016/j.hydromet.2021.105705>.
- Yasa, S., Aydin, O., Al-Bujasim, M., Birol, B., Gencten, M., 2023. Recycling valuable materials from the cathodes of spent lithium-ion batteries: A comprehensive review. *J. Energy Storage* 73, 109073. <https://doi.org/10.1016/j.est.2023.109073>.
- Yi, A., Zhu, Z., Liu, Y., Zhang, J., Su, H., Qi, T., 2021. Using highly concentrated chloride solutions to leach valuable metals from cathode-active materials in spent lithium-ion batteries. *Rare Met.* 40, 1971–1978. <https://doi.org/10.1007/s12598-020-01503-4>.
- Zeng, X., Li, J., Shen, B., 2015. Novel approach to recover cobalt and lithium from spent lithium-ion battery using oxalic acid. *J. Hazard. Mater.* 295, 112–118. <http://dx.doi.org/10.1016/j.jhazmat.2015.02.064>.
- Zhang, K., Liang, H., Zhong, X., Cao, H., Wang, R., Liu, Z., 2022. Recovery of metals from sulfate leach solutions of spent ternary lithium-ion batteries by precipitation with phosphate and solvent extraction with P507. *Hydrometallurgy* 210, 105861. <https://doi.org/10.1016/j.hydromet.2022.105861>.
- Zhang, L., Lijuan, L., Rui, H., Shi, D., Peng, X., Ji, L., Song, X., 2020. Lithium recovery from effluent of spent lithium battery recycling process using solvent extraction. *J. Hazard. Mater.* 398, 122840. <https://doi.org/10.1016/j.jhazmat.2020.122840>.
- Zhao, H., Chang, J., Boika, A., Bard, A.J., 2013. Electrochemistry of high concentration copper chloride complexes. *Anal. Chem.* 85, 7696–7703. <https://doi.org/10.1021/ac4016769>.
- Zheng, X., Gao, W., Zhang, X., He, M., Lin, X., Cao, H., Zhang, Y., Sun, Z., 2017. Spent lithium-ion battery recycling – Reductive ammonia leaching of metals from cathode scrap by sodium sulphite. *Waste Manage.* 60, 680–688. <http://dx.doi.org/10.1016/j.wasman.2016.12.007>.
- Zhu, P., Gastol, D., Marshall, J., Sommerville, R., Goodship, V., Kendrick, E., 2021. A review of current collectors for lithium-ion batteries. *J. Power Sources* 485, 229321. <https://doi.org/10.1016/j.jpowsour.2020.229321>.

Zou, Y., Chernyaev, A., Ossama, M., Seisko, S., Lundström, M., 2024a. Leaching of NMC industrial black mass in the presence of LFP. *Sci. Rep.* 14, 10818.
<https://doi.org/10.1038/s41598-024-61569-3>.

Zou, Y., Chernyaev, A., Seisko, S., Sainio, J., Lundström, M., 2024b. Removal of iron and aluminum from hydrometallurgical NMC-LFP recycling process through precipitation. *Miner. Eng.* 218, 109037.
<https://doi.org/10.1016/j.mineng.2024.109037>.

Business, Economy
Art, Design, Architecture
Science, Technology
Crossover

| Doctoral Theses

Aalto DT 28/2025

ISBN 978-952-64-2393-7

ISBN 978-952-64-2394-4 (pdf)

Aalto University
School of Chemical Engineering
Department of Chemical and Metallurgical
Engineering
aalto.fi